

MENTHOL INHIBITS 5-HT<sub>3</sub> RECEPTOR-MEDIATED CURRENTS

Abrar Ashoor, Jacob C. Nordman, Daniel Veltri, Keun-Hang Susan Yang, Yaroslav Shuba, Lina Al Kury, Bassem Sadek, Frank C. Howarth, Amarda Shehu, Nadine Kabbani and Murat Oz

Laboratory of Functional Lipidomics, Departments of Pharmacology (AA, B.S., LAK, MO) and Physiology (FCH), College of Medicine and Health Sciences, UAE University, Al Ain, UAE, Department of Molecular Neuroscience (JCN, NK), School of Systems Biology (DV), Department of Computer Science (AS), George Mason University, 4400 University Drive, Fairfax, VA 22030, USA, International Center of Molecular Physiology of the National Academy of Sciences of Ukraine, Kiev, Ukraine (YS), Department of Biological Sciences, Schmid College of Science and Engineering, Chapman University, One University Drive, Orange, CA 92866, USA (KHSY).

JPET #203976

Running title: Menthol on 5-HT<sub>3</sub> receptor

Correspondence address:

Murat Oz M.D., Ph.D.

Laboratory of Functional Lipidomics,  
Department of Pharmacology and Therapeutics,  
College of Medicine and Health Sciences,  
UAEU, Al Ain, UAE.

E-mail: Murat\_Oz@uaeu.ac.ae

Number of text pages: 46

Number of tables: 1

Number of figures: 8

Number of references: 39

Number of words in the abstract: 206

Number of words in the introduction: 413

Number of words in the discussion: 1337

**ABBREVIATIONS:** 5-HT, 5-hydroxytryptamine; ANOVA, analysis of variance; BAPTA, 1,2-bis (*o*-aminophenoxy) ethane-*N, N, N', N'*-tetraacetic acid; DMSO, dimethyl sulfoxide; GR65630, 3-(5-methyl-1H-imidazol-4-yl)-1-(1-methylindol-3-yl)propan-1-one; HEPES, 4-(2-hydroxyethyl) piperazineethane sulfonic acid; MBS, modified Barth's solution; MDL72222, Tropanyl 3,5-dichlorobenzoate; PMSF, phenylmethylsulfonyl fluoride, PTX, pertussis toxin.

### Abstract

The effects of alcohol monoterpene menthol, a major active ingredient of the peppermint plant was tested on the function of human hydroxytryptamine type 3 (5-HT<sub>3</sub>) receptors expressed in *Xenopus* oocytes. 5-HT (1 μM)-evoked currents recorded by two-electrode voltage clamp technique were reversibly inhibited by menthol in a concentration-dependent (IC<sub>50</sub>=163 μM) manner. The effects of menthol developed gradually, reaching a steady-state level within 10-15 min, and did not involve G-proteins, since GTP-γ-S activity remained unaltered and the effect of menthol was not sensitive to pertussis toxin pretreatment. The actions of menthol were not stereoselective since (-), (+), and racemic menthol inhibited 5-HT<sub>3</sub> receptor mediated currents to the same extent. Menthol inhibition was not altered by intracellular BAPTA injections and trans-membrane potential changes. The maximum inhibition observed for menthol was not reversed by increasing concentrations of 5-HT. Furthermore, specific binding of 5-HT<sub>3</sub> antagonist [3H]GR65630 was not altered in the presence of menthol (up to 1 mM), indicating that menthol acts as a noncompetitive antagonist of 5-HT<sub>3</sub> receptor. Finally, 5-HT<sub>3</sub> receptor mediated currents in acutely dissociated nodose ganglion neurons were also inhibited by menthol (100 μM). These data demonstrate that menthol, at pharmacologically relevant concentrations, is an allosteric inhibitor of 5-HT<sub>3</sub> receptors.

## **Introduction**

Menthol is among the world's most important flavoring agents and is used in a variety of commercial products such as toothpaste, mouthwash, foods, cigarettes, and oral pharmaceutical preparations (Eccles, 1994; Patel et al., 2007). Menthol is a monocyclic terpene alcohol that occurs naturally in more than 100 essential oils, including spearmint and peppermint. Discovery of menthol activation of transient receptor potential melastatin subfamily channel 8 (TRPM8) was a major breakthrough in understanding the molecular mechanisms underlying menthol's cooling action (Jordt et al, 2003). Besides its importance in cool sensation, menthol is the major active ingredient of various herbal medicines. Since antiquity, peppermint (a major constituent of which is menthol) has been used widely for various medicinal purposes ranging from management of musculoskeletal pain and the common cold to the treatment of gastrointestinal disorders such as nausea, vomiting and irritable bowel syndrome (for reviews, Grigoleit and Grigoleit, 2005; Cappello et al., 2007; Patel et al., 2007; Haniadka et al., 2012). However, the cellular and molecular targets mediating the beneficial effects of peppermint and other menthol containing products on gastrointestinal disorders are currently unknown (De Araújo et al., 2011).

The serotonin type three (5-HT<sub>3</sub>) receptor, a member of the cys-loop family of ligand-gated ion channels, mediates fast depolarizing actions of 5-HT in the central and peripheral nervous system (Yakel and Jackson, 1988). 5-HT<sub>3</sub> receptors are also expressed by enteric sensory neurons in the mucosal layer and in the nerve cell body of interneurons and motor neurons in the enteric nervous system (Galligan, 2002). The peristaltic reflex

can be initiated by release of 5-HT following stimulation of enterochromaffine cells by pressure or other intraluminal stimulus and subsequent stimulation through 5-HT<sub>3</sub> receptors of ganglionic and synaptic transmission in the myenteric plexus. Involvement of 5-HT<sub>3</sub> receptors in nausea, vomiting, and irritable bowel syndrome has been well established (for reviews, Riering et al., 2004; Faerber et al., 2007). In fact, antagonists of 5-HT<sub>3</sub> receptor are currently one of the most effective therapeutic agents in treatment of chemotherapy-induced nausea, vomiting, and irritable bowel syndrome (for a review, Thompson and Lummis, 2007). Interestingly, there is considerable overlap between the gastrointestinal actions of menthol and 5-HT<sub>3</sub> receptor antagonists. Therefore, it is likely that some of the actions of menthol involve modulation of 5-HT<sub>3</sub> receptor function.

In this study, using electrophysiological and biochemical methods, we have investigated the effect of menthol on the functional properties of human 5-HT<sub>3</sub> receptors expressed in *Xenopus* oocyte and 5-HT<sub>3</sub> receptors of rat nodose ganglion neurons.

## Methods

Mature female *Xenopus laevis* frogs were purchased from *Xenopus laevis* I, Ann Arbor, MI and were housed in dechlorinated tap water at 18 °C and fed with dry frog pellets at least twice a week. Clusters of oocytes were removed surgically under benzocaine (Sigma, St.Louis, MO) anesthesia (0.03 % w/v). Individual oocytes were manually dissected away in a solution containing (in mM): NaCl, 88; KCl, 1; NaHCO<sub>3</sub>, 2.4; MgSO<sub>4</sub>, 0.8; HEPES, 10 (pH 7.5) and stored for 2-7 days in modified Barth's solution (MBS) containing (in mM): NaCl 88; KCl 1; NaHCO<sub>3</sub> 2.4; CaCl<sub>2</sub>; 2; MgSO<sub>4</sub> 0.8; HEPES 10 (pH 7.5), supplemented with sodium pyruvate 2 mM, penicillin 10,000 IU/L, streptomycin 10 mg/L, gentamicin 50 mg/L, and theophylline 0.5 mM. Oocytes were placed in a 0.2 ml recording chamber and superfused at a constant rate of 3-5 ml/min. The bathing solution consisted of : 95 mM NaCl; 2 mM KCl; 2 mM CaCl<sub>2</sub>; and 5 mM HEPES 5 (pH 7.5). 5-HT<sub>3A</sub> receptor cRNA (3 ng) was injected into each oocyte. After two days, cells were impaled with two standard glass microelectrodes filled with a 3 M KCl (1-3 MΩ). The oocytes were routinely voltage clamped at a holding potential of -70 mV using GeneClamp-500B amplifier (Axon Instruments Inc., Burlingame, CA). Current responses were digitized by A/D converter and analyzed using pClamp 8 (Axon Instruments Inc., Burlingame, CA) or Origin™ (Originlab Corp. Northampton, MA), run on an IBM/PC. Current-voltage curves were generated by 2 s voltage ramps between -120 to +20 mV. Oocyte capacitance was measured by a paired-ramp method described earlier (Oz et al., 2004a). Briefly, voltage-ramps were employed to elicit constant capacitive current ( $I_{cap}$ ), and the charge associated with this current was calculated by the

integration of  $I_{cap}$ . Ramps had slopes of 2 V/s and durations of 20 ms and started at a holding potential of  $-90$  mV. A series of 10 paired-ramps was delivered at 1 s intervals and averaged traces were used for charge calculations. In each oocyte, the averages of 5-6 measurements were used to obtain values for membrane capacitance ( $C_m$ ). Currents for  $I_{cap}$  recordings were filtered at 20 kHz and sampled at 50 kHz. Current density was calculated by normalizing the average of three consecutive control currents to the oocyte capacitance.

Compounds were applied by addition to the superfusate. All chemicals used in preparing the solutions were from Sigma-Aldrich (St. Louis, MO). BAPTA, 5-HT, and MDL72222 (Tropanyl 3, 5-dichlorobenzoate) were purchased from Tocris Cookson (St. Louis, MO). Procedures for the injections of BAPTA (50 nl, 100 mM) were performed as described previously (Oz et al., 1998). Injections were performed 10 min prior to recordings using oil-driven ultra microsyringe pumps (Micro4, WPI, Inc. Sarasota, FL). Stock solutions of menthol were prepared in ethanol. Vehicle (ethanol) alone did not affect 5-HT<sub>3</sub> receptor function when added at concentrations as high as 0.3 % (v/v), a concentration twice greater than the most concentrated application of the agents used. Electrophysiological recordings from oocytes were conducted 2 days after cRNA injections.

**Synthesis of cRNA:** The cDNA clone of the human 5-HT<sub>3A</sub> and 5-HT<sub>3B</sub> subunits were provided by OriGen Inc. (Rockville, MD). Complementary RNAs (cRNAs) were synthesized *in vitro* using a mMessage mMachine RNA transcription kit (Ambion Inc., Austin, TX). The quality and sizes of synthesized cRNAs were confirmed by denatured

RNA agarose gels.

**Radioligand Binding Studies:** Oocytes were injected with 10 ng human 5-HT<sub>3</sub> cRNA and functional expression of the receptors was assessed by electrophysiology on day three. Isolation of oocyte membranes was carried out by modification of a method described earlier (Oz et al., 2004b). Briefly, oocytes were suspended (20  $\mu$ l/oocyte) in a homogenization buffer (HB) containing HEPES 10 mM, EDTA 1 mM, 0.02 % NaN<sub>3</sub>, 50  $\mu$ g/mL bacitracin, and 0.1 mM PMSF (pH 7.4) at 4 °C on ice and homogenized using a motorized Teflon homogenizer (six strokes, 15 s each at high speed). The homogenate was centrifuged for 10 min at 800 g. The supernatant was collected and the pellet was resuspended in HB and re-centrifuged at 800 g for 10 min. Supernatants were then combined and centrifuged for 1 h at 36,000 g. The membrane pellet was resuspended in HB at the final protein concentration of 0.5 - 0.7 mg/ml and used for the binding studies.

Binding assays were performed in 500  $\mu$ L of 10 mM HEPES (pH 7.4) containing 50  $\mu$ L of oocyte preparation and 1 nM [<sup>3</sup>H]GR65630 (58.7 Ci/mmol; Perkin-Elmer, Inc. Waltham, MA). Nonspecific binding was determined using 100  $\mu$ M MDL72222. Oocyte membranes were incubated with [<sup>3</sup>H]GR65630 in the absence and presence of menthol at 4 °C for 1 h before bound radioligand was separated by rapid filtration onto GF/B filters presoaked in 0.3 % polyethylenimine. Filters were then washed with two 5 mL washes of ice-cold HEPES buffer and left in 3 mL of scintillation fluid for at least 4 h before scintillation counting was conducted to determine amounts of membrane-bound radioligand.

**[<sup>35</sup>S]GTP $\gamma$ S binding:** Oocyte membranes for [<sup>35</sup>S]GTP $\gamma$ S binding experiments

were prepared as described earlier (Lipinsky and Oron, 1996). 150 oocytes were gently homogenized at 4°C by passing through a 27 gauge needle in 4 ml of homogenization medium (in mM: NaCl 5, Na-HEPES 5, PMSF 0.6, and leupeptin 4 pM, pH 7.5). The homogenate was centrifuged for 5 sec in a conical centrifuge tube at 8,000 g. The supernatant was decanted from the precipitated cellular organelles and the procedure repeated. Following the aspiration of the lipid layer at the surface of the supernatant, it was centrifuged for 20 min at 8,000 g. The particulate pellet was resuspended by re-homogenization in 1.8 ml of binding medium (in mM: KCl 80, Na-HEPES 20, MgCl<sub>2</sub> 1, PMSF 1.7, and leupeptin 0.013, pH 7.5). Each tube contained (in 25 µl volume) the following: Membrane preparation equivalent to 1 oocyte and the following additions (in mM): KCl 45, Na-HEPES 11, MgCl<sub>2</sub> 0.5, PMSF 1.0, leupeptin 7.3 pM. pH=7.5 and [<sup>35</sup>S]GTPγS 0.5 nM-10 pM. [<sup>35</sup>S]GTPγS (1,000-1,500 Ci/mmol) was from New England Nuclear (Boston, MA). Non-specific binding was assayed by adding 0.5 mM non-radioactive GTPγS and 50 µM ATP. The mixture was incubated at room temperature (22 °C) for 30 min and filtered rapidly through Whatman (Clifton, NJ) GFIC 25 mm filters and washed with 5 ml of ice-cold wash solution (in mM: KCl 80, Na-HEPES 20, MgCl<sub>2</sub> 1, pH 7.5). The filters, once washed, were subjected to scintillation counting.

**Whole cell patch-clamp recording:** Nodose ganglion neurons were acutely isolated from adult male Sprague-Dawley rats (200-300 g) as described earlier (Yang et al., 2010). Briefly, nodose ganglia were rapidly dissected, minced, and dissociated by incubation in type III trypsin (0.75 mg/ml; Sigma), type IA collagenase (1.25 mg/ml; Sigma), and DNase IV (0.125 mg/ml; Sigma) in Dulbecco's modified Eagle's medium

(pH 7.4) at 35 °C for 25 min. Type I-S soybean trypsin inhibitor (1.25 mg/ml; Sigma) was added to stop enzymatic digestion.

The whole cell patch-clamp technique was employed with an Axopatch-1C amplifier and pCLAMP8 software (Axon Instruments Inc., Burlingame, CA). Neurons were held at -60 mV holding potential and superfused at room temperature (22-24 °C) with extracellular solution containing (in mM) 150 NaCl, 5 KCl, 2.5 CaCl<sub>2</sub>, 1 MgCl<sub>2</sub>, HEPES, 10 glucose. Patch electrodes (2-5 MΩ) were filled with an internal solution containing (in mM) 140 KCl, 2 MgCl<sub>2</sub>, 1 CaCl<sub>2</sub>, 11 EGTA, 10 HEPES, 2 ATP, pH 7.4. Serotonin- containing solutions (with or without drug) were delivered by gravity flow from a linear barrel array consisting of fused silica tubes (i.d. = 200 μm) connected to independent reservoirs; rapid solution exchanges (<50 msec) were achieved by shifting the pipette horizontally using a micromanipulator. The neuron under study was placed within 50 μm of the opening of these tubes and exposed to the desired solution. Culture dishes containing neurons were continuously perfused at 1-2 ml/min with normal external solution. Menthol was diluted in external solution and applied through a gravity- driven perfusion system.

**Obtaining a Structural Model of 5-HTR3A:** We used the iterative threading assembly refinement (I-TASSER) server (Zhang, 2008) to generate a structural model for 5-HTR3A. To utilize the server, protocols outlined by Roy et al. (2010) were closely followed. Chain A of the nicotinic acetylcholine receptor (nAChR), under PDB ID: 2BG9 (Miyazawa et al., 2003), was chosen as the modeling template for a Cys-loop receptor

(Thompson et al., 2010). A confidence score (C-Score) was associated by I-TASSER (Roy et al., 2010). The top-scoring model (with C-Score of -2.08) was chosen as a good model for chain A. The top-scoring structure for chain A was aligned with TM-Align (Zhang Y and Skolnick J., 2005) with each of the separate nAChR chains in order to obtain the same pentameric symmetry in nAChR. The result was a modeled structure for each of the chains, or the complete pentameric structure in 5-HTR3A. Only the transmembrane domain of the modeled structure was employed for docking, as described below.

**Docking of L-menthol on the 5-HTR3A Structural Model:** AutoDock 4.2 (Morris et al., 2009) was used to perform rigid docking simulations along with Molecular Graphics Laboratory Tools (MGLTools) Vr. 1.5.4 rev. 30 (Sanner et al., 1999; Morris et al., 2009; Sanner et al., 2002). Both ligand and receptor files were prepared using recommended procedures described in the MGLTools software documentation (<http://mgltools.scripps.edu/documentation>). Two torsion angles were specified as parameters for the ligand, while the receptor was modeled as a rigid structure. A grid box area was specified for AutoDock to bind the ligand on relevant regions of the receptor's molecular surface. Choice of the specified grid box area took into account similar binding characteristics believed to be shared by propofol and menthol (Hall et al., 2011) and the close homology of the gamma-aminobutyric acid alpha receptor (GABA<sub>A</sub>R) to 5-HTR3A (Thompson et al., 2010). Accordingly, the grid box was set to include key residue positions evaluated by Williams and Akabas (2002) for testing propofol binding to the

GABA<sub>A</sub>R- $\alpha_1$  segment. These positions were mapped onto the 5-HTR3A sequence through a multiple sequence alignment using ClustalW 2.1 (Larkin et al., 2007). Once the grid box area was set to include these residues, docking simulations were performed in AutoDock using the Lamarckian Genetic Algorithm under default parameters. In order to obtain convergence, the “maximum number of evaluations” was increased to “long.” MGLTools was used for analysis of the generated docked configurations for the ligand.

**Data analysis:** For the nonlinear curve fitting and regression fits of the radioligand binding data, the computer software Origin<sup>TM</sup> (Originlab Corp. Northampton, MA) was used. In functional assays, average values were calculated as mean  $\pm$  standard error means (S.E.M.). Statistical significance was analyzed using ANOVA or Student's *t* test and post hoc Bonferroni test was used following ANOVA. Concentration-response curves were obtained by fitting the data to the logistic equation,

$$y = \{ (E_{\max} - E_{\min}) / (1 + [x/EC_{50}]^n) \} + E_{\min},$$

where *x* and *y* are concentration and response, respectively,  $E_{\max}$  is the maximal response,  $E_{\min}$  is the minimal response,  $EC_{50}$  is the half-maximal concentration, and *n* is the slope factor.

## Results

Bath application of the specific 5-HT<sub>3</sub> receptor agonists 2-methyl-5-HT (10 μM) caused activation of fast inward currents only in oocytes injected with cRNA transcribed from cloned cDNA encoding human 5-HT<sub>3</sub> receptors (data not shown, n=12). Currents activated by 1 μM 5-HT were completely inhibited by 0.1 μM LY278584, a specific antagonist of 5-HT<sub>3</sub> receptor, further indicating that the 5-HT induced current responses were mediated by the 5-HT<sub>3</sub> receptor-ion channel complex (n=7).

In our initial studies, (-)-menthol, the most widely occurring isomer in natural sources (Eccles, 1994), was tested. Continuous bath application of (-)-menthol (300 μM) for 15 min did not affect membrane resistance ( $R_m$ ), membrane capacitance ( $C_m$ ), or resting membrane potential ( $V_m$ ) in oocytes expressing human 5-HT<sub>3</sub> receptor. Summary of results were presented in table 1.

Figure 1A presents recordings of 5-HT (1 μM)-induced currents in control conditions (on the *left*), after 15 min application of (-)-menthol (100 μM, in the *middle*), and after 20 min. of washout period (on the *right*). Time course of the effects of (-)-menthol application on the maximal amplitudes of 5-HT-induced currents from 5-7 oocytes are presented in Figure 1B. In the presence of vehicle (0.3% v/v ethanol), the maximal amplitudes of 5-HT induced currents remained unaltered during the experiments lasting 45-60 min (controls). However, in the presence of 100 μM (-)-menthol, the maximal current amplitudes decreased gradually, reaching to steady-state levels within 10 to 15 min. Recovery from menthol effect was slow and usually incomplete during the 15 min washout period (Figure 1B).

In the next series of experiments, we examined the concentration-response relationship of the menthol effect on 5-HT<sub>3</sub> receptors (Figure 1C). The threshold concentration for inhibition by menthol was 30  $\mu$ M and maximal inhibition was achieved in concentrations ranging between 1 to 3 mM. The inhibition of 5-HT (1  $\mu$ M)-induced current by 15 min menthol application was concentration-dependent with an IC<sub>50</sub> of 163  $\pm$  14  $\mu$ M and a slope value of 1.2 (Figure 1C). Some of the biological actions of menthol have been shown to be stereospecific (Eccles, 1994). For this reason, we compared the effects of 100  $\mu$ M of (-), (+), and racemic ( $\pm$ ) menthol on human 5-HT<sub>3</sub> receptor. Results indicated that they all similarly inhibited the 5-HT<sub>3</sub> receptors and there were no statistically significant differences in the inhibition caused by these compounds (Figure 1D; n=6-8, ANOVA,  $P > 0.05$ ). In the remaining experiments unless stated otherwise, racemic ( $\pm$ ) menthol was employed.

In earlier studies, participation of G-protein coupled receptors (Galeotti et al., 2002) and direct involvement of G-proteins (Klasen et al., 2012; Zhang et al., 2012) in menthol-induced cellular and behavioral responses have been reported. Thus, we tested the effect of menthol in control (distilled-water injected) and pertussis toxin (PTX) - injected oocytes expressing 5-HT<sub>3</sub> receptors. There was no significant difference in menthol inhibition of 5-HT responses between controls and PTX-injected cells (Figure 2A, n=5-7, ANOVA,  $P > 0.05$  for the significance of menthol inhibition between controls and PTX group). We have also conducted experiments to investigate the effect of menthol (300  $\mu$ M) on the specific binding of [<sup>35</sup>S]GTP $\gamma$ S in oocyte membranes. Equilibrium curves for the binding of [<sup>35</sup>S]GTP $\gamma$ S in the presence and absence of

menthol are presented in figure 2B (n= 8-9). Menthol did not significantly change the specific binding of [<sup>35</sup>S]GTPγS. Maximum binding activities (B<sub>max</sub>) of [<sup>35</sup>S]GTPγS were 6.4 ± 0.4 and 6.9 ± 0.6 pmole/oocyte (means ± SEM) for controls and menthol, respectively. The apparent affinity (K<sub>D</sub>) of the receptor for [<sup>35</sup>S]GTPγS was 0.91 ± 0.2 and 1.0 ± 0.2 μM for controls and menthol, respectively. There was no statistically significant difference between control and menthol treated groups with respect to both K<sub>D</sub> (ANOVA, n=8-9, *P*>0.05) and the B<sub>max</sub> values (ANOVA, n=8-9, *P*>0.05).

In the concentration range used in this investigation, menthol has been shown to increase intracellular Ca<sup>2+</sup> levels in a wide range of cells in a TRPM8-receptor independent manner, including skeletal muscle sarcoplasmic reticulum (Palade, 1987, Neumann and Copello, 2011, EC<sub>50</sub> = 938 μM-1 mM), tracheal epithelial cells (Takeuchi et al., 1994, 100 μM-1 mM) human leukemia cells (Lu et al., 2006; 25 to 100 μM) and dorsal horn neurons (Tsuzuki et al., 2004, 100 μM-1 mM). Therefore we investigated the effect of the Ca<sup>2+</sup> chelator BAPTA on menthol inhibition of 5-HT responses. In oocytes injected with BAPTA, the inhibition of 5-HT responses by 15 min menthol (300 μM) application was not significantly different from controls (Figure 2C; ANOVA, n=5-6, *P* > 0.05; significance of menthol effect between distilled water- injected and BAPTA-injected group).

The mechanisms of menthol actions were further investigated using different application modes of 5-HT and menthol. If menthol acts as an open-channel blocker, it must be present during the channel opening in order to access its binding site(s). In other words, the extent of menthol inhibition would be independent of its pre-incubation time.

However, the extent of inhibition by menthol was significantly enhanced with prolongation of its pre-incubation time (Figure 3A). During these experiments, coapplication of 5-HT and menthol without menthol pre-incubation was considered as zero point and the menthol inhibition was plotted as a function of pre-incubation time. Close examination of the time course of menthol actions indicated that the inhibition occurs at fast and slow phases with the respective time constants of  $\tau_{1/2\text{fast}} = 4.2$  sec. and  $\tau_{1/2\text{slow}} = 3.4$  min. Presentation of menthol during constant 5-HT application also induced a rapidly developing inhibition that is consistent with the fast component of menthol inhibition (Figure 3B). Time course of the recovery from menthol inhibition was considerably slower, within the solution exchange time of the recording system. Interestingly, menthol (300  $\mu\text{M}$ ) pre-incubation alone, without its co-application with 5-HT, also caused a significant inhibition of the 5-HT-induced currents (Figure 3C). Menthol pre-incubation alone, did not cause a significant change of desensitization, measured from linearly decaying portion of 5-HT induced currents presented in Figure 3C. Half desensitization time ( $\tau_d$ ) was  $10.2 \pm 1.4$  sec and  $9.7 \pm 0.8$  sec, in the absence and presence of menthol (paired *t*-test,  $n=5$ ;  $P<0.05$ ).

Without menthol pre-incubation, co-application of 5-HT (1  $\mu\text{M}$ ) and menthol (300  $\mu\text{M}$ ) also inhibited the maximal amplitudes of currents. In the presence of menthol, there was a significant increase in desensitization of 5-HT-induced current (Figure 3D). A small tail current was also noticeable after the cessation of menthol+5-HT co-application.

Recent electrophysiological studies reported that menthol inhibits the functions of

Na<sup>+</sup> (Gaudioso et al., 2011; Pan et al., 2012) and Ca<sup>2+</sup> channels (Pan et al., 2012) in a voltage-dependent manner. The effect of changing membrane potential relationship between 5-HT-activated current and membrane potential before and after 10 min. menthol (300 μM) application is shown in figure 4A. Examination of the voltage-dependence of the menthol actions indicated that the degree of the inhibition of the 5-HT (1 μM)-induced currents tended to increase with depolarizing membrane potentials (Figure 4B). Compared to -120 mV, difference in the extent of menthol inhibition reached to statistically significant levels at 0 and +20 mV (n=6-7; paired *t*-test, *P*<0.05). The small tail current observed after the cessation of menthol+5-HT co-application (Figure 3D), together with a relatively weak voltage dependence of menthol inhibition, is in agreement with open channel blockade. However, due to possible variations in solution-exchange time and drug application speeds among different oocyte recordings and difficulties inherent to oocyte expression system, we were not able to record and analyze these tail currents consistently.

Considering the time courses of menthol actions (Figure 3A), we hypothesized that two binding site(s) with fast and slow kinetics may differentially contribute to voltage-dependency of menthol inhibition. For this purpose, we have compared the extent of voltage-dependent inhibition at two time-points; without pre-incubation (during co-application of 5-HT + menthol) and after 10 min menthol pre-incubation. Without pre-incubation, the extent of menthol inhibition at depolarized membrane potentials was significantly elevated. For example, compared to -120 mV, menthol inhibition at +20 mV was  $18 \pm 2$  % higher (n=4-5). However, following 10 min pre-incubation, this difference

was reduced significantly to  $3 \pm 1$  % (paired *t*-test,  $n=4-5$ ,  $P<0.05$ ).

Menthol may alter 5-HT<sub>3</sub> receptor function via competitive inhibition of 5-HT binding to the receptor. To examine this possibility, the concentration-response curve of 5-HT was examined in the absence and presence of 300 μM menthol. The EC<sub>50</sub> values in the absence and presence of menthol were  $1.2 \pm 0.2$  and  $3.2 \pm 0.3$  μM (means  $\pm$  S.E.M.), respectively ( $n=5-7$ ). As shown in figure 5A, menthol did not significantly alter EC<sub>50</sub> values and inhibited the maximal 5-HT-responses to the same percentage of control values, suggesting that menthol is a noncompetitive inhibitor of 5-HT<sub>3</sub> receptors. In radioligand binding experiments, 5-HT concentration-dependently inhibited the specific binding of 1 nM [<sup>3</sup>H]GR65630 (Figure 5B). The concentration-dependent inhibition of [<sup>3</sup>H]GR65630 binding by 5-HT was not altered by 300 μM menthol (Figure 5B). The IC<sub>50</sub> values in the absence and presence of menthol were  $561 \pm 169$  and  $639 \pm 177$  nM, respectively (ANOVA,  $n=8-11$ ;  $P>0.05$ ). Similarly, increasing menthol concentrations did not reduce specific [<sup>3</sup>H]GR65630 binding to membranes of oocytes expressing 5-HT<sub>3</sub> receptor cDNA (Figure 5C).

Menthol does not appear to alter agonist displacement of 5-HT<sub>3</sub> antagonist binding, suggesting no change in agonist affinity. Interpretation of radioligand studies is complicated by the fact that radioligand binding is performed under conditions in which receptors are predominantly in the desensitized/high affinity state (for a discussion Lovinger and Zhou, 1993). However, agonist binding is not independent of channel state since open and desensitized receptors are necessarily agonist bound, and thus any effect that stabilizes these states may alter apparent agonist affinity. Electrophysiological

studies in various types of mammalian cells (Lovinger and Zhou, 1993) and oocyte expression system (Oz et al., 2003) indicate that in contrast to 5-HT, dopamine (DA) gates 5-HT<sub>3</sub> receptors with low efficacy because peak currents evoked by receptor-saturating concentrations of DA are significantly smaller than those evoked by 5-HT. Therefore, in this study, we used the inefficacious 5-HT<sub>3</sub> agonist DA (1 mM) to resolve the effects of menthol on 5-HT<sub>3</sub> receptor agonist binding affinity and channel gating efficacy. We compared the effect of menthol between 5-HT and DA responses. The inhibition of DA-induced currents by 15 min menthol (300 μM) application was not significantly different from controls (Figure 5D; n=5-6, ANOVA;  $P < 0.05$ ; significance of menthol effect between DA and 5-HT-activated currents).

Monoterpenes such as menthol and thymol display close structural similarities to propofol (Watt et al., 2008). Furthermore, menthol and propofol share general anesthetic activity and common interaction sites for activation of GABA<sub>A</sub> receptors (Watt et al., 2008; Zhang et al., 2008). In fact, recent studies indicated that the mutations causing decreased propofol actions on GABA<sub>A</sub> receptors also affect menthol potentiation of these receptors (Watt et al., 2008). In an attempt to identify chemical moieties which modulate the inhibitory effect of menthol, we divided the compounds into two subgroups, namely the unsubstituted congeners, cyclohexane and eucalyptol, and the OH-substituted derivatives, menthol and propofol. Within the unsubstituted derivatives, cyclohexane was the least active one, showing an inhibition potency of less than 5% at 100 μM application. Similarly, the ether derivative eucalyptol with increased lipophilic character appeared to exhibit detectable increase in its potency when compared with cyclohexane,

suggesting that the presence of hydrogen-accepting oxygen might contribute in modulating the inhibitory affinity of eucalyptol with the 5HT<sub>3A</sub> receptor protein (Figure 6A). In contrast, an introduction of aliphatic hydroxyl group as present in menthol or even an aromatic one in propofol potentially enhanced their inhibitory effect on 5-HT<sub>3A</sub> receptor, thus significantly increased the inhibition observed for menthol as well as propofol in the current study (Figure 6A). Inhibition by these compounds increased in the order of cyclohexane>eucalyptol>menthol>propofol (Figure 6A).

We have next investigated whether cyclohexane, eucalyptol, menthol, and propofol interacts functionally on the 5-HT<sub>3</sub> receptor (Figure 6B). In this set of experiments, the effects of compounds were tested within the same cell to minimize the variations between cells. Bath application of 100  $\mu$ M cyclohexane alone (for 15 min) did not affect the maximal amplitudes of 5-HT-induced current. However, the inhibitory effect of menthol was enhanced significantly in the co-presence of cyclohexane and menthol (Figure 6B,  $n=6$ , ANOVA,  $P<0.05$ ). In agreement with earlier findings (Rusch et al., 2007), propofol inhibited 5-HT<sub>3</sub> receptors. However, there was no statistically significant difference between the extent of inhibition caused by co-application of menthol and propofol or the sum of the inhibitory actions of menthol alone and propofol alone (Figure 6B). Similarly only additive action (neither occlusive nor synergistic actions) was observed for menthol and eucalyptol co-applications (Figure 6B), suggesting that other than cyclohexanol, there is no functional interaction among the binding sites of propofol, eucalyptol, and menthol.

Subunit composition of 5-HT<sub>3</sub> receptors has been shown to influence modulation

of the receptor function by various drugs (Thompson and Lummis, 2007; Barnes et al., 2011). Therefore, we have tested whether the co-expression of A and B subtypes would alter the extent of menthol inhibition. Results indicated that the difference in the extent of menthol inhibition was not statistically significant between 5-HT<sub>3A</sub> and 5-HT<sub>3AB</sub> receptor subtypes (n=5-7, ANOVA,  $P>0.05$ ; Figure 7A).

In the next set of experiments, we investigated whether menthol acts on 5-HT<sub>3</sub> receptors expressed natively in neuronal structures. For this purpose, we have tested the effect of 100  $\mu$ M menthol on 5-HT<sub>3</sub> receptor-mediated currents recorded in acutely dissociated adult rat nodose ganglion neurons. Figure 7 illustrates a decrease in the amplitude of 5-HT (10  $\mu$ M)-induced currents by 15 min bath application of 100  $\mu$ M menthol. In seven neurons tested, the average inhibition by 100  $\mu$ M menthol application was  $61 \pm 7\%$  (Figure 7B). Menthol in 100  $\mu$ M and higher concentrations caused a slowly developing (within a minute) inward current in approximately 40 % (5/12) of the nodose ganglion neurons tested, and these neurons were not included in the present study. Responses to menthol applications have been described in earlier studies in these neurons and suggested to be due to activations of TRPM8 and TRPA1 receptors (Fajardo et al., 2008).

A bioinformatics procedures to evaluate L-menthol (1R,2S,5R) binding to the 5-HT<sub>3</sub> receptor was utilized. A structure for the L-menthol ligand (ZINC ID: 01482164) was obtained from the ZINC Vr. 12 Database (Irwin et al., 2012). In choosing the 5-HT<sub>3A</sub> sequences, a longer 516aa human isoform (Uniprot AC: P46098-5) was considered in order to include several splice variants. A docking method was used to test

for L-menthol direct binding to the predicted 5-HT<sub>3</sub> receptor structure. Fig. 8A shows key residues for the association of the L-menthol ligand, identified through a multiple sequence alignment of the 5-HT<sub>3</sub> receptor (see Methods). These key residues, which were used to define the area of interest for docking through the grid specification mechanism, are annotated by the red triangle at THR361 in Fig. 8A. Position THR361 appears directly involved in the interaction between menthol and nACh receptor (used to model the cys loop receptor as described in Methods). Since our modeling procedure to obtain a structure for the 5-HT<sub>3</sub> receptor uses the existing alpha 7 nACh receptor crystal structure as a template, it is to be expected that structural similarity may result in similar binding sites for menthol between the 5-HT<sub>3</sub> receptor and the nACh receptor. Indeed, our docking simulations for L-menthol on 5-HTRA resulted in a number of low-energy configurations for L-menthol that were stabilized by interactions with THR361. This particular docked configuration of the ligand is shown circled in black, in two different viewing angles in Fig. 8B panel 1 (top-down view) and panel 2 (side view). Figure 8B (panels 3 and 4) demonstrate that an h-bond between menthol and THR361 (at a distance of 1.81 Å) stabilizes the ligand onto the predicted receptor structure. MGLTools analysis reports a binding energy of -6.35 kcal/mol for this ligand configuration, suggesting that residue THR361 plays a central role in L-menthol binding to 5-HT<sub>3</sub> receptors. A number of docking simulations also resulted in low-energy configurations that placed the ligand in contact with residue ASP266 (data not shown). The two predicted residues, THR361 and ASP266, might thus constitute a naturally occurring binding site for menthol on 5-HT<sub>3</sub> receptors.



## Discussion

The results indicate that menthol reversibly inhibits the function of human 5-HT<sub>3</sub> receptors expressed in *Xenopus* oocytes in a concentration- dependent manner with IC<sub>50</sub> value of 163 μM. The results of both electrophysiological and radioligand binding studies indicated that menthol does not compete with the 5-HT binding site on the receptor.

In earlier studies, participation of G-protein coupled receptors such as kappa-opioid receptors (Galeotti et al., 2002) and direct involvement of G-proteins (Klasen et al., 2012; Zhang et al., 2012) in menthol- induced cellular and behavioral responses have been reported. However, the results indicate that activity of G-proteins remained unchanged in the presence of menthol. Menthol has been shown to increase intracellular Ca<sup>2+</sup> levels and activate various Ca<sup>2+</sup> sensitive kinases (Farco and Grundmann, 2012). In oocyte expression system, alterations in intracellular Ca<sup>2+</sup> levels can be examined indirectly by monitoring the holding current under voltage-clamp conditions since Ca<sup>2+</sup>-activated Cl<sup>-</sup> channels in oocytes are highly sensitive to Ca<sup>2+</sup> (for reviews Dascal, 1988). However, menthol application alone (up to 1 mM at room temperature of 21-23 °C) did not induce changes in holding currents, suggesting that menthol did not alter intracellular Ca<sup>2+</sup> levels in *Xenopus* oocytes. Furthermore, menthol continued to inhibit 5-HT<sub>3</sub> receptors to a similar extent in BAPTA-injected oocytes, further suggesting that changes in intracellular Ca<sup>2+</sup> levels are not involved in menthol inhibition of 5-HT<sub>3</sub>-receptors.

Menthol, as a result of its lipophilic character, preferentially partitions from an aqueous phase into membrane structures (Trombetta et al., 2005; Turina et al., 2006). Partitioning of these lipophilic substances has been suggested to result in increased

membrane fluidity, permeability, and disturbance of membrane integrity. However, passive membrane properties such as membrane capacitance, resting membrane potential, and oocyte input resistance were not significantly influenced by menthol (Table 1), suggesting that in the concentrations used in this study, menthol did not disrupt the integrity of the lipid membrane.

Our results provide the first demonstration that menthol directly inhibits the function of human 5-HT<sub>3</sub> receptors in clinically relevant concentrations. In a recent study (Heimes et al., 2011), 5-HT-induced [<sup>14</sup>C]guanidinium influx mediated by natively expressed voltage-sensitive Na<sup>+</sup> channels and 5-HT<sub>3</sub> receptors in NIE-115 cells (Barann et al., 1999) was significantly inhibited by menthol (estimated IC<sub>50</sub> value is in the range of 100-300 μM), further suggesting that menthol can modulate the function of 5-HT<sub>3</sub> receptor. Similarly, in rat ileum smooth muscle (Heimes et al., 2011), 5-HT-induced muscle contractures thought to be mediated by 5-HT<sub>3</sub> receptors were also suppressed by menthol (with an estimated IC<sub>50</sub> value of 200-600 μM). In agreement with these findings in rodents, our patch-clamp studies in rat nodose ganglion neurons also indicate that menthol inhibits 5-HT<sub>3</sub>-receptor- mediated currents. Although actions of several drugs have been reported to be modulated by subunit combinations (for reviews, Thompson and Lummis, 2007; Barnes et al., 2011), there was no statistically significant difference of menthol inhibition between 5-HT<sub>3A</sub> and 5-HT<sub>3AB</sub> receptors in our study.

In earlier studies, menthol in the concentration ranges used in this study has been shown to act directly on GABA-A (Pan et al., 2012; EC<sub>50</sub>= 1.1 mM), glycine (Hall et al., 2004; 100-300 μM), and ryanodine receptors (Palade, 1987; Neumann and Copello,

2012,  $EC_{50} = 1$  mM). Both ligand-gated and voltage-gated channels are inhibited by menthol (Pan et al., 2012;  $IC_{50} = 297$   $\mu$ M for  $Na^+$  channels and  $IC_{50}$  of 125  $\mu$ M  $Ca^{2+}$  channels in dorsal horn neurons). Moreover, the effective concentrations observed in the current study were found to be comparable with menthol concentrations sufficient to activate TRPM8 channels with  $EC_{50}$  values ranging between 67-196  $\mu$ M (McKemy et al., 2002; Sherkheli 2010) in *Xenopus* oocytes. However; menthol also nonselectively activates TRPV3 ( $EC_{50}$  20 mM), inhibits mouse TRPA1 ( $IC_{50}$  68  $\mu$ M) (Macpherson et al., 2006). In our study, the concentration of menthol effective on 5-HT<sub>3</sub> receptors ranged from 30  $\mu$ M to 1 mM ( $IC_{50} = 163$   $\mu$ M). These concentrations approximate those used in human psychophysical studies and are considerably lower than those used in over-the-counter products ( $\approx$ 500 mM) (Yosipovitch et al., 1996; Namer et al., 2005). Menthol taken orally is effectively absorbed in gastrointestinal mucosa and can easily reach the range of menthol concentrations used in this study. Menthol undergoes extensive enterohepatic recirculation, and it is rapidly but incompletely (about 50%) metabolized to menthol glucuronide, which is excreted both in the bile and in the urine (Gelal et al., 1999). In a recent study, a high concentration of menthol (54  $\mu$ g/g) was detected in brain tissue at 5 min after 100 mg/kg intraperitoneal injection (Pan et al., 2012), indicating that menthol is rapidly absorbed into the brain. Therefore, functional modulation of 5-HT<sub>3</sub> receptors demonstrated in this study can mediate some of the pharmacological actions of menthol.

Menthol is known to act stereoselectively in some, but not all, *in vivo* and *in vitro* assay systems (for reviews: Eccles, 1994; Farco and Grundmann, 2012). In an earlier

study, Hall et al (2004) showed that the effect of menthol on GABA<sub>A</sub> currents were stereoselective, with (+)-menthol being more potent than (-)-menthol, while menthol modulation of glycine-receptors did not display stereospecificity. In our study, we could not detect a stereoselectivity of menthol actions on 5-HT<sub>3</sub> receptor (Figure 1).

Allosteric modulators alter the functional properties of ligand-gated-ion channels by interacting with site(s) that are topographically distinct from the ligand binding sites (for a review; Onaran and Costa, 2009). In electrophysiological studies, although the potency of the 5-HT, a natural ligand (agonist) for this receptor, was not altered, its efficacy was significantly inhibited by menthol, indicating that menthol does not compete with the 5-HT binding site on the receptor. In agreement with these findings, radioligand binding studies indicated that displacement of [<sup>3</sup>H]GR65630 (competitive antagonists of 5-HT<sub>3</sub> receptors) by 5-HT was not significantly affected by menthol, further suggesting that menthol does not interact with the 5-HT binding site on the human 5-HT<sub>3</sub> receptor. In an earlier report on NG101 cell lines (Heimes et al., 2011), menthol did not affect the radioligand binding site on the 5-HT<sub>3</sub> receptor. Similarly 5-HT (up to 0.1 mM tested in this study) did not affect specific binding of [<sup>32</sup>H]-menthol to membranes from guinea-pig lung (Wright et al., 1998). In an earlier study, binding of [<sup>32</sup>H]-Flunitrazepam to GABA<sub>A</sub> receptors in primary cultures of mouse cortical neurons was not affected by up to 1 mM concentrations of menthol (Garcia et al., 2006). The results of functional studies together with radioligand binding experiments suggest that menthol does not compete with the 5-HT binding site, but it acts as an allosteric inhibitor of the 5-HT<sub>3</sub> receptor.

In recent studies, menthol in the concentration range used in this study has been

reported to be an allosteric modulator of GABA<sub>A</sub> (Hall et al., 2004) and  $\alpha 4\beta 2$  nicotinic receptors (Hans et al., 2012) i.e., menthol binds to site(s) topographically distinct from the agonist sites on these receptor. Under physiological conditions, the non-competitive property of the allosteric menthol inhibition may be advantageous since the increases in concentration of endogenous agonist (5-HT) in the synaptic cleft to millimolar concentrations cannot alter the efficacy of menthol on the receptor. Dopamine competes with 5-HT binding site, but activates these receptors with lower efficacy and cause a considerably less desensitization. Since a saturating concentration of dopamine was used in the present study, menthol inhibition could not have resulted from fewer number of channels in desensitized state or from a decrease in agonist affinity.

Based on the kinetics of menthol effect (the fast and slow components of inhibition in Figure 3A), it is likely that multiple allosteric binding sites are involved in the interaction of this molecule with the 5-HT<sub>3</sub> receptor. In agreement with this hypothesis, co-application of 5-HT and menthol (Figures 3A and 3C), without pre-incubation, also induce a fast inhibition of 5-HT-induced currents by blocking the channel pore or promoting the desensitization of the receptor (Dopico and Lovinger, 2009).

Open-channel blockade is a widely used model to describe the inhibition of functions of various ion channels. Tail currents seen after the cessation of menthol application and, although weak, a voltage-sensitivity of its action are in favor of open channel inhibition. However, open-channel model cannot account for all of the findings of the present study. First, for open channel blockers, the presence of the agonist is

required to let the blocker enter the channel after the receptor was opened by the agonist. However pre-incubation of menthol caused significant further inhibition (Figures 1A and 3A), indicating the compound can also interact with the closed state of the 5-HT<sub>3</sub> receptor. Second, the proportion of somewhat weak voltage-sensitivity of menthol inhibition observed at the early phase of the menthol diminished significantly after 10 min menthol incubation.

Menthol, a highly lipophilic agent, first dissolves into the lipid membrane (Turina et al., 2006) and then diffuses into a non-annular lipid space to inhibit the ion channel-receptor complex (Sanghvi et al., 2009). Consistent with this idea, the effect of menthol on 5-HT<sub>3</sub> receptor reached a maximal level within 10-15 min of application. Similarly, actions of several hydrophobic allosteric modulators (McCool and Lovinger, 1995; Oz et al., 2002a, b) on 5-HT<sub>3</sub> receptors require several minutes (5-20 min) of application time to reach their maxima (for a review Oz, 2006), suggesting that the binding site(s) for these allosteric modulators is located inside the lipid membrane and that drug exposure time rather than channel opening is essential for menthol inhibition of the receptor. Thus, it appears that menthol can interact with 5-HT<sub>3</sub> receptors during the closed state. Overall, it is likely that at least two binding sites mediate menthol actions on 5-HT<sub>3</sub> receptor. One of the sites is either causing open channel blockade or promoting desensitization of the receptor (Dopico and Lovinger, 2009) and is weakly sensitive to transmembrane electric field. Another binding site located in the bilayer lipid membrane (Trombetta et al., 2005; Turina et al., 2006) has access to closed state of channel-receptor complex and diminishes the percent contribution of voltage-sensitive binding site to the total amount

of inhibition.

It is plausible that menthol reduces current amplitude by lowering the energy barrier for receptors to enter a desensitized and/or closed state(s). This mechanism has already been proposed for nicotinic receptors (Spivak et al., 2007). Clearly, further investigations in which receptor kinetics can be studied in a more detailed and precise manner are required to delineate the mechanisms of menthol actions on 5-HT<sub>3</sub> receptor function.

Evaluation of the data in Figure 6 provided evidence that combining menthol with either eucalyptol or propofol enhanced its inhibitory effect on 5HT-induced currents, suggesting that these compounds have additive effects on 5-HT<sub>3</sub> receptors (Figure 6B). On the other hand, cyclohexane (100 μM) alone displayed undetectable efficacy at inhibiting 5HT<sub>3A</sub> receptors, but increased significantly the potency of menthol, suggesting that cyclohexane may facilitate the interaction of menthol with its binding site on the receptor (Figure 6B). Our results also indicate that, the extent of 5HT<sub>3</sub> receptor inhibition varied with the substitution pattern on the cyclohexane skeleton and an aromatic hydroxyl group as present in propofol has the highest potency in inhibiting 5HT<sub>3A</sub> receptor. The results observed for the parent compound cyclohexane and derivatives thereof may be useful in further understanding the molecular mechanisms involved in pharmacological effects of menthol as well as propofol.

Menthol is a monoterpenoid and other monoterpenoids such as borneo, thymol, menthone, camphor, and carvone has been shown to potentiate GABA-A and glycine receptors (Priestley et al., 2003; Hall et al., 2004). In an earlier study camphor has also

been shown to inhibit nicotinic receptor-induced norepinephrine secretion and  $\text{Ca}^{2+}$  increases in bovine adrenal chromaffin cells (Park et al., 2001).

In conclusion, our results indicate that menthol inhibits the function of homomERICALLY expressed human 5-HT<sub>3</sub> receptor by a noncompetitive mechanism. These data add to a growing body of evidence (Farco and Grundmann, 2012) suggesting that in addition to TRPM8 receptors, other target proteins such as 5-HT<sub>3</sub> receptors can also contribute to the pharmacological actions of menthol.

**Acknowledgement:** The authors thank Dr. David Lovinger of NIAAA/IRP for his constructive comments and valuable suggestions. The authors also thank Dr. Mary Pfeiffer of NIDA/IRP for her careful editing of the manuscript.

**Authorship contribution:**

Participated in research design: Shuba Y.; Susan Yang, K.H.; Shehu A.; Kabbani, N.; Sadek B.; Howarth, F.C. Oz, M.

Conducted experiments: Ashoor A.; Nordman, J.C.; Veltri, D., Al Kury, L.,

Contributed new reagents or analytic tools: Shehu A.; Susan Yang, K.H.; Veltri D.,

Performed data analysis: Ashoor A.; Nordman, J.C.; Veltri, D., Al Kury, L., Kabbani, N.; Shehu, A.; Oz, M.

Wrote or contributed to the writing of the manuscript: Ashoor, A.; Oz, M.; Kabbani N, Shehu A.

## References

Barann M, Göthert M, Brüß M, Bönisch H. (1999) Inhibition by steroids of [14C]-guanidinium flux through the voltage-gated sodium channel and the cation channel of the 5-HT<sub>3</sub> receptor of N1E-115 neuroblastoma cells. *Naunyn Schmiedebergs Arch Pharmacol.* 360: 225-233.

Barnes NM, Hales TG, Lummis SC, Peters JA. (2009) The 5-HT<sub>3</sub> receptor--the relationship between structure and function. *Neuropharmacology.* 56: 273-284.

Berman HM, Westbrook J, Feng Z, Gilliland G, Bhat TN, Weissig H, Shindyalov IN, Bourne PE. (2000) The Protein Data Bank *Nucleic Acids Research*, 28: 235-242.

Cappello G, Spezzaferro M, Grossi L, Manzoli L, Marzio L. (2007) Peppermint oil (Mintoil) in the treatment of irritable bowel syndrome: a prospective double blind placebo-controlled randomized trial. *Dig Liver Dis.* 39:530-536.

Dascal N (1987) The use of *Xenopus* oocytes for the study of ion channels. *CRC Crit Rev Biochem* 22:317–387.

De Araújo DA, Freitas C, Cruz JS. (2011). Essential oils components as a new path to understand ion channel molecular pharmacology. *Life Sci.* 89:540-544.

Dopico AM, Lovinger DM. (2009) Acute alcohol action and desensitization of ligand-gated ion channels. *Pharmacol Rev.* 61: 98-114

Eccles R. (1994) Menthol and related cooling compounds. *J Pharm Pharmacol.* 46: 618-630.

Faerber L, Drechsler S, Ladenburger S, Gschaidmeier H, and Fischer W (2007) The neuronal 5-HT<sub>3</sub> receptor network after 20 years of research--evolving concepts in management

of pain and inflammation. *Eur J Pharmacol* 560:1-8.

Fajardo O, Meseguer V, Belmonte C, Viana F. (2008) TRPA1 channels mediate cold temperature sensing in mammalian vagal sensory neurons: pharmacological and genetic evidence. *J Neurosci.* 28: 7863-7875.

Farco JA, Grundmann O. (2012) Menthol - pharmacology of an important naturally medicinal "cool." *Mini Rev Med Chem.* 13:124-131.

Ford AC, Talley NJ, Spiegel BM, Foxx-Orenstein AE, Schiller L, Quigley EM, Moayyedi P. (2008) Effect of fibre, antispasmodics, and peppermint oil in the treatment of irritable bowel syndrome: systematic review and meta-analysis. *BMJ.* 337: a2313.

Galeotti N, Di Cesare Mannelli L, Mazzanti G, Bartolini A, Ghelardini C. (2002) Menthol: a natural analgesic compound. *Neurosci Lett.* 322:145-148.

Galligan JJ. (2002) Ligand-gated ion channels in the enteric nervous system. *Neurogastroenterol Motil* 14: 611-623.

Gelal A, Jacob P 3rd, Yu L, Benowitz NL. (1999) Disposition kinetics and effects of menthol. *Clin Pharmacol Ther.* 66:128-135.

Grigoleit HG, Grigoleit P. (2005) Gastrointestinal clinical pharmacology of peppermint oil. *Phytomedicine.* 12:607-611.

Gaudio C, Hao J, Martin-Eauclaire MF, Gabriac M, Delmas P. (2012) Menthol pain relief through cumulative inactivation of voltage-gated sodium channels. *Pain.* 153: 473-484.

Hall AC, Turcotte CM, Betts BA, Yeung WY, Agyeman AS, Burk LA. (2004) Modulation of human GABAA and glycine receptor currents by menthol and related monoterpenoids. *Eur J Pharmacol.* 506: 9-16.

Hall AC, Griffith TN, Tsikolia M, Kotey FO, Gill N, Humbert DJ, Watt EE, Yermolina YA, Goel S, El-Ghendy B and Hall CD. (2008) Cyclohexanol analogues are positive modulators of GABA(A) receptor currents and act as general anaesthetics in vivo. *Eur. J. Pharmacol* 667:175-181.

Haniadka R, Popouri S, Palatty PL, Arora R, Baliga MS. (2012) Medicinal plants as antiemetics in the treatment of cancer: a review. *Integr. Cancer Ther.* 11:18-28.

Hans M, Wilhelm M, Swandulla D. (2012) Menthol Suppresses Nicotinic Acetylcholine Receptor Functioning in Sensory Neurons via Allosteric Modulation. *Chem Senses.* 37: 463-469.

Hawthorn M, Ferrante J, Luchowski E, Rutledge A, Wei XY, and Triggle DJ (1988) The actions of peppermint oil and menthol on calcium channel dependent processes in intestinal, neuronal and cardiac preparations. *Aliment Pharmacol Ther* 2:101–118.

Heimes K, Hauk F, Verspohl EJ. (2011) Mode of action of peppermint oil and (-)-menthol with respect to 5-HT<sub>3</sub> receptor subtypes: binding studies, cation uptake by receptor channels and contraction of isolated rat ileum. *Phytother Res.* 25: 702-708.

Hills JM, Aaronson PI. (1991) The mechanism of action of peppermint oil on gastrointestinal smooth muscle. An analysis using patch clamp electrophysiology and isolated tissue pharmacology in rabbit and guinea pig. *Gastroenterology.* 101: 55-65.

Humphrey W, Dalke A and Schulten K. (1996) VMD - Visual Molecular Dynamics. *J. Molec. Graphics* 14:33-38.

Irwin J, Sterling T, Mysinger M, Bolstad E and Coleman R. (2012) ZINC: A Free Tool to Discover Chemistry for Biology. *Journal of Chemical Information and Modeling.* 52:1757-

1768.

Journigan VB and Zaveri NT. (2012) TRPM8 ion channel ligands for new therapeutic applications and as probes to study menthol pharmacology. *Life Sci*, in press

Klasen K, Hollatz D, Zielke S, Gisselmann G, Hatt H, Wetzel CH. (2012) The TRPM8 ion channel comprises direct Gq protein-activating capacity. *Pflugers Arch*. 463: 779-797.

Knowlton WM, McKemy DD. (2011) TRPM8: from cold to cancer, peppermint to pain. *Curr Pharm Biotechnol*. 12:68-77.

Larkin MA, Blackshields G, Brown NP, Chenna R, McGettigan PA, McWilliam H, Valentin F, Wallace IM, Wilm A, Lopez R, Thompson JD, Gibson TJ, Higgins DG. (2007) Clustal W and Clustal X version 2.0. *Bioinformatics* 23:2947-2948.

Lu HF, Hsueh SC, Yu FS, Yang JS, Tang NY, Chen SC, Chung JG. (2006). The role of Ca<sup>2+</sup> in (-)-menthol-induced human promyelocytic leukemia HL-60 cell death. *In Vivo*. 20: 69-75.

Macpherson LJ, Hwang SW, Miyamoto T, Dubin AE, Patapoutian A, Story GM. (2006) More than cool: promiscuous relationships of menthol and other sensory compounds. *Mol Cell Neurosci*. 32:335-343.

Mahieu F, Owsianik G, Verbert L, Janssens A, De Smedt H, Nilius B, Voets T. (2007) TRPM8-independent menthol-induced Ca<sup>2+</sup> release from endoplasmic reticulum and Golgi. *J Biol Chem*. 282:3325-36.

McCool BA, Lovinger DM. (1995) Ifenprodil inhibition of the 5-hydroxytryptamine<sub>3</sub> receptor. *Neuropharmacology*. 34: 621-629.

McKay DL, Blumberg JB. (2006) A review of the bioactivity and potential health

benefits of peppermint tea (*Mentha piperita* L.). *Phytother Res.* 20: 619-633.

Michel F, Sanner MF. (1999) Python: A Programming Language for Software Integration and Development. *J. Mol. Graphics Mod.* 17:57-61.

Miyazawa A, Fujiyoshi Y and Unwin N. (2003) Structure and gating mechanism of the acetylcholine receptor pore. *Nature* 424:949-955.

Morales M, Wang SD. (2002) Differential composition of 5-hydroxytryptamine<sub>3</sub> receptors synthesized in the rat CNS and peripheral nervous system. *J. Neurosci.* 22: 6732-6741.

Morris GM, Huey R, Lindstrom W, Sanner, MF, Belew RK, Goodsell DS and Olson AJ. (2009) Autodock4 and AutoDockTools4: automated docking with selective receptor flexibility. *J. Computational Chemistry* 16:2785-91.

Namer, B., Seifert, F., Handwerker, H.O., Maihofner, C., 2005. TRPA1 and TRPM8 activation in humans: effects of cinnamaldehyde and menthol. *NeuroReport* 16: 955- 959.

Neumann JT, Copello JA. (2011) Cross-reactivity of ryanodine receptors with plasma membrane ion channel modulators. *Mol Pharmacol.* 80: 509-517.

Onaran HO and Costa T (2009) Allosteric coupling and conformational fluctuations in proteins. *Curr Protein Pept Sci* 10:110-115.

Oz M (2006) Receptor-independent actions of cannabinoids on cell membranes: focus on endocannabinoids. *Pharmacol Ther* 111:114-144.

Oz M, Soldatov NM, Melia MT, Abernethy DR, and Morad M (1998) Functional coupling of human L-type Ca<sup>2+</sup> channel and angiotensin AT<sub>1</sub>A receptor coexpressed in *Xenopus* oocytes. *Mol Pharmacol* 54:1106-1112.

Oz M, Zhang L, Rotondo A, Sun H, Morales M. (2003) Direct activation by dopamine of recombinant human 5-HT<sub>1A</sub> receptors: comparison with human 5-HT<sub>2C</sub> and 5-HT<sub>3</sub> receptors. *Synapse*. 50:303-313.

Oz M, Zakharova IO, Dinc M, and Shippenberg T (2004b) Cocaine inhibits cromakalim activated K<sup>+</sup> currents in follicle-enclosed oocytes. *Naunyn-Schmiedeberg's Arch Pharmacol* 369:252-259.

Oz M, Zhang L, Morales M. (2002a) Endogenous cannabinoid, anandamide, acts as a noncompetitive inhibitor on 5-HT<sub>3</sub> receptor-mediated responses in *Xenopus* oocytes. *Synapse*. 46:150-156

Oz M, Zhang L, and Spivak CE (2002b) Direct noncompetitive inhibition of 5-HT<sub>3</sub> receptor-mediated responses by forskolin and steroids. *Arch Biochem Biophys* 404:293-301.

Palade P. (1987) Drug-induced Ca<sup>2+</sup> release from isolated sarcoplasmic reticulum. II. Releases involving a Ca<sup>2+</sup>-induced Ca<sup>2+</sup> release channel. *J Biol Chem* 262:6142-6148.

Pan R, Tian Y, Gao R, Li H, Zhao X, Barrett JE, Hu H. (2012) Central Mechanisms of Menthol-induced Analgesia. *J. Pharmacol. Exp. Ther.* 343: 661-672.

Park TJ, Seo HK, Kang BJ, Kim KT. (2001) Noncompetitive inhibition by camphor of nicotinic acetylcholine receptors. *Biochem Pharmacol.* 61:787-793.

Patel T, Ishiujji Y, Yosipovitch G. (2007) Menthol: a refreshing look at this ancient compound. *J Am Acad Dermatol.* 57:873-878.

Priestley CM, Williamson EM, Wafford KA, Sattelle DB. (2003) Thymol, a constituent of thyme essential oil, is a positive allosteric modulator of human GABA(A) receptors and a homo-oligomeric GABA receptor from *Drosophila melanogaster*. *Br J Pharmacol.* 140:1363-

Riering K, Rewerts C, and Zieglgänsberger W (2004) Analgesic effects of 5-HT<sub>3</sub> receptor antagonists. *Scand J Rheumatol* 119:19-23.

Roy A, Kucukural A, Zhang Y. (2010) I-TASSER: a unified platform for automated protein structure and function prediction. *Nature Protocols* 5:725-738.

Rüsch D, Braun HA, Wulf H, Schuster A, Raines DE. (2007) Inhibition of human 5-HT<sub>3A</sub> and 5-HT<sub>3AB</sub> receptors by etomidate, propofol and pentobarbital. *Eur J Pharmacol.* 573: 60-64.

Sanner M, Stoffler D and Olson AJ. ViPEr a Visual Programming Environment for Python. In *Proceedings of the 10th International Python Conference*, pg. 103-115.

Sanghvi M, Hamouda AK, Davis MI, Morton RA, Srivastava S, Pandhare A, Duddempudi PK, Machu TK, Lovinger DM, Cohen JB, Blanton MP. (2009) Hydrophobic photolabeling studies identify the lipid-protein interface of the 5-HT<sub>3A</sub> receptor. *Biochemistry.* 48: 9278-9286.

Sherkheli MA, Vogt-Eisele AK, Bura D, Beltrán Márques LR, Gisselmann G, and Hatt H. (2010) Characterization of selective TRPM8 ligands and their structure activity response (S.A.R) relationship. *J Pharm Pharm Sci.* 13:242-253.

Takeuchi S, Tamaoki J, Kondo M, Konno K. (1994) Effect of menthol on cytosolic Ca<sup>2+</sup> levels in canine airway epithelium in culture. *Biochem Biophys Res Commun.* 201:1333-1338.

Tate S. (1997) Peppermint oil: a treatment for postoperative nausea. *J Adv Nurs.* 26:543-549.

Thompson AJ and Lummis SC (2007) The 5-HT<sub>3</sub> receptor as a therapeutic target. *Expert*

Opin Ther Targets 11:527-540.

Thompson A., Lester H. and Lummis S. (2010) The structural basis of function in Cys-loop receptors. Quarterly Reviews of Biophysics 43:449-499.

Turina AV, Nolan MV, Zygadlo JA, Perillo MA. (2006) Natural terpenes: self-assembly and membrane partitioning. Biophys Chem. 122:101-113.

Watt EE, Betts BA, Kotey FO, Humbert DJ, Griffith TN, Kelly EW, Veneskey KC, Gill N, Rowan KC, Jenkins A, Hall AC. (2008) Menthol shares general anesthetic activity and sites of action on the GABA(A) receptor with the intravenous agent, propofol. Eur J Pharmacol. 590: 120-126.

Westfall RE. 2004. Use of anti-emetic herbs in pregnancy: women's choices, and the question of safety and efficacy. Complement Ther Nurs Midwifery 10: 30-36.

Williams DB, Akabas MH. (2002) Structural evidence that propofol stabilizes different GABAA receptor states at potentiating and activation concentrations. J. Neuroscience 22:7417-7424.

Wright C.E., Bowen W.P., Grattan T.J., and Morice A.H. (1998) Identification of the L-menthol binding site in guinea-pig lung membranes. Brit. J. Pharmacol. 123, 481-486.

Yakel JL and Jackson MB (1988) 5-HT<sub>3</sub> receptors mediate rapid responses in cultured hippocampus and a clonal cell line. Neuron 1:615-621.

Yang KH, Isaev D, Morales M, Petroianu G, Galadari S, Oz M. (2010a) The effect of  $\Delta^9$ -tetrahydrocannabinol on 5-HT<sub>3</sub> receptors depends on the current density. Neuroscience. 171:40-49.

Yang KH, Galadari S, Isaev D, Petroianu G, Shippenberg TS, Oz M. (2010b) The nonpsychoactive cannabinoid cannabidiol inhibits 5-hydroxytryptamine<sub>3A</sub> receptor-mediated currents in *Xenopus laevis* oocytes. *J Pharmacol Exp Ther.* 333: 547-554.

Yosipovitch G, Szolar C, Hui XY, Maibach H. (1996) Effect of topically applied menthol on thermal, pain and itch sensations and biophysical properties of the skin. *Arch Dermatol Res.* 288: 245-248.

Zhang X, Mak S, Li L, Parra A, Denlinger B, Belmonte C, McNaughton PA. (2012) Direct inhibition of the cold-activated TRPM8 ion channel by  $G\alpha_q$ . *Nat Cell Biol.* 14:851-858.

Zhang XB, Jiang P, Gong N, Hu XL, Fei D, Xiong ZQ, Xu L, Xu TL. (2008) A-type GABA receptor as a central target of TRPM8 agonist menthol. *PLoS One.* 3(10): e3386.

Zhang, Y. (2008) I-TASSER server for protein 3D structure prediction. *BMC Bioinformatics* 9(40).

Zhang Y and Skolnick J. (2005) TM-align: A protein structure alignment algorithm based on TM-Score. *Nucleic Acids Research* 33:2302-2309.

**Footnotes:** This study was in part supported by the funds from intramural research program of NIDA/NIH, USA and the UAEU Research Funds. Research in our laboratory is also supported by LABCO, partner of Sigma-Aldrich.

**Figure legends**

**Figure 1.** The effect of menthol on 5-HT<sub>3</sub> receptor-mediated ion currents. **(A)** Records of currents activated by 1  $\mu$ M 5-HT in control (*left*), coapplication of 100  $\mu$ M (-)-menthol and 5-HT after 15 min (-)-menthol application (*middle*), 20 min wash-out (*right*). **(B)** Time-course of the effect of menthol on the currents induced by 1  $\mu$ M 5-HT at 5 min intervals. The maximal amplitudes of currents were normalized to first agonist application (at time 0) for each experiment. Solid bar represents application time for vehicle (ethanol, 0.3%) and menthol (100  $\mu$ M). Data points represent means  $\pm$  S.E.M. of 7-8 cells. **(C)** Concentration-response curve for menthol inhibition of 5-HT<sub>3</sub> receptor-mediated ion currents. For all concentrations used, menthol was applied for 15 min. Data points are the mean  $\pm$  S.E.M. (n=5-7); error bars not visible are smaller than the size of the symbols. The curve is the best fit of the data to the logistic equation described in the Methods. **(D)** Comparison of the extent of inhibition caused by 300  $\mu$ M of (+), (-), and racemic forms of menthol application for 15 min. Bars represent the means  $\pm$  S.E.M. from 5 to 7 cells.

**Figure 2.** Effects of menthol on 5-HT<sub>3</sub> receptor-mediated currents in pertussis toxin injected oocytes and on [<sup>35</sup>S]GTP $\gamma$ S binding of oocyte membranes. **(A)** The effect of 100  $\mu$ M menthol application (15 min) on the maximal amplitudes of 5-HT-induced currents in oocytes injected with 50 nl distilled-water, controls (n=6) or 50 nl of pertussis toxin (PTX; 50  $\mu$ g/ml, n=7). Bars represent the means  $\pm$  S.E.M. **(B)** The effect of 300  $\mu$ M menthol on [<sup>35</sup>S]GTP $\gamma$ S binding to oocyte membrane preparation. Membranes were

incubated with different concentrations of [ $^{35}$ S]GTP $\gamma$ S for 30 min at room temperature, and the results analyzed as described in *Materials and Methods*. Data points for controls and menthol are indicated by *filled* and *open circles*, respectively (n=7-8). **(C)** Bar presentation of the effects of 1  $\mu$ M menthol application (20 min) on the maximal amplitudes of 5-HT-induced currents in oocytes injected with 50 nl distilled-water, controls (n=5) or BAPTA (50 nl, 200 mM, n=7). Bars represent the means  $\pm$  S.E.M.

**Figure 3.** The effect of increasing menthol preincubation time and different menthol application modes on the 5-HT $_3$  receptor-mediated currents. **(A)** Time-course of menthol inhibition as a function of menthol preincubation time. Solid curve shows a best fit for the data points; an exponential decay with two time constants  $\tau_{fast}$  and  $\tau_{slow}$ , is shown in the figure. Each data point represents the means  $\pm$  SEM from 7-8 oocytes. **(B)** The effect of introducing 300  $\mu$ M menthol after activation of currents by 5-HT (1  $\mu$ M). Solid grey bar on the top of the current trace represents the 5-HT application time. Duration of menthol application indicated with solid black bar was presented below current trace. Small transient current fluctuation before the menthol application is due to change between two 5-HT application tubes to test the contribution of a possible mechanical artifact during solution exchange in the chamber. Calibration bars were indicated in the panel. **(C)** The effect of menthol application before and after 5-HT application. Menthol (300  $\mu$ M) application time was indicated with solid grey bars. Menthol was present in the bath only before and after, but not during, 5-HT application. **(D)** The effect of menthol and 5-HT coapplication, without a menthol preincubation on the 5-HT $_3$  receptor mediated

currents. Menthol was applied only in the presence of 5-HT.

**Figure 4.** The effect of membrane potential changes on menthol inhibition of 5-HT<sub>3</sub> receptor-mediated ion currents. **(A)** Current-voltage relationship of 5-HT-activated current in the absence (black trace) and presence (grey trace) of 300 μM menthol. Currents were activated by 1 μM 5-HT in the same oocyte. **(B)** Percentage inhibition of 5-HT-activated current by 300 μM menthol at different membrane potentials; there are no significant differences among these values at different membrane potentials ( $P > 0.05$ , ANOVA;  $n = 5$ ). **(C)** Time-dependent alterations in the voltage-dependency of menthol inhibition. Current traces in response to voltage ramps were recorded within one minute co-application of 5-HT and menthol and compared to those recorded after 10 min of menthol application ( $P < 0.05$ , ANOVA;  $n = 6$ )

**Figure 5.** The effect of menthol on 5-HT concentration-response curves and the specific binding of [<sup>3</sup>H]GR65630 on *Xenopus* oocytes expressing 5-HT<sub>3</sub> receptors. **(A)** Concentration-response curves for 5-HT-activated current in the absence (*filled circles*) and presence (*open circles*) of 300 μM menthol. Currents were activated by 5-HT concentrations ranging from 0.1 to 100 μM. Menthol was applied for 20 min, and 5-HT and menthol were then co-applied for 10 to 15 sec. Data points are the mean ± S.E.M. ( $n = 5-6$ ). The curve is the best fit of the data to the logistic equation described in the methods. The control concentration-response curve is normalized to the maximal response. The concentration-response curve in the presence of menthol is the percentage

of the maximal control. **(B)** Inhibition of specific [<sup>3</sup>H]GR65630 binding by nonlabeled 5-HT in membranes after 1 hour pre-incubation with 300 μM menthol. The concentration of [<sup>3</sup>H]GR65630 was 1 nM. The inhibition curve shows pooled data from 8-11 measurements from 3 experiments. **(C)** Effects of increasing concentration of menthol on the specific binding of [<sup>3</sup>H]GR65630. Experiments were conducted in the presence of 1 nM of [<sup>3</sup>H]GR65630. The results present data from 8-11 measurements. Data points indicate mean ± S.E.M. **(D)** Comparison of the effect of 15 min. application of 300 μM menthol on the maximal amplitudes of currents induced by 5-HT (1 μM) and dopamine (1 mM). There was no statistically significant difference among the bars (ANOVA, n=7-8,  $P>0.05$ ).

**Figure 6.** Comparison of the effects of some compounds structurally related to menthol on the 5-HT<sub>3</sub> receptors. **(A)** Comparison of the effects of equimolar concentrations (100 μM) of cyclohexane, eucalyptol, propofol, and menthol on 5-HT<sub>3</sub> receptors. Bars represent the means ± S.E.M (n=5-8). Chemical structures of the compounds were presented at the top of each bar. **(B)** Comparison of the interaction between menthol and other structurally similar compounds on the currents activated by 5-HT in the same oocytes. Bars represent the means ± S.E.M (n=5-6)

**Figure 7.** The effect of menthol on A and AB subunit combination of human 5-HT<sub>3</sub> receptors expressed in *Xenopus* oocytes and 5-HT-induced currents recorded in acutely dissociated nodose ganglion neurons. **(A)** Comparison of the effect of 100 μM menthol

on the human 5-HT<sub>3A</sub> and 5-HT<sub>3AB</sub> receptors expressed in oocytes. Bar graph shows average inhibition (mean  $\pm$  SEM) of 5-HT (1  $\mu$ M)-induced currents by 15 min menthol application in 5-7 oocytes. **(B)** Records are sequential (from *left to right*) current traces obtained from a single nodose ganglion neuron voltage-clamped at -60 mV. Currents activated by 3  $\mu$ M 5-HT before (on the *left*), after 10 min application of 100  $\mu$ M menthol (in the *middle*) and recovery of 5-HT-induced current after 15 min of washout period (on the *right*).

**Figure 8.** **(A)** A multiple sequence alignment obtained with ClustalW 2.1 between the human GABA<sub>A</sub>R- $\alpha_1$  subunit (UniProt AC: P14867), the alpha 7 nACh receptor chain A (Miyazawa et al., 2003; PDB ID: 2BG9), and the human 5-HT<sub>3</sub> receptor (UniProt AC: P46098-5). Boxed and shaded regions indicate key residue positions from the M3 segment of GABA<sub>A</sub>R- $\alpha_1$  evaluated by Williams and Akabas (2002) for propofol binding. Docking simulations show L-menthol binding at the position indicated by the red triangle. **(B)** Panels 1 and 2: A bioinformatics model of the pentameric structure for the 5-HT<sub>3</sub> receptor (top-down view in panel 1 and side-view in panel 2), with nAChR drawn in translucent gray for reference. All 5-HT<sub>3</sub> receptor chains are of the same primary sequence; chain letters refer to the nAChR receptor chains with which the modeled chain for 5-HTR3A was aligned to obtain the pentameric symmetry for 5-HTR3A. Chain A is colored in orange, B in cyan, C in green, D in violet, and E in red. The binding site for the ligand is circled in black. Panels 3 and 4: A representative lowest-energy (-6.35 kcal/mol) configuration for the L-menthol ligand in two different views. The h-bond that

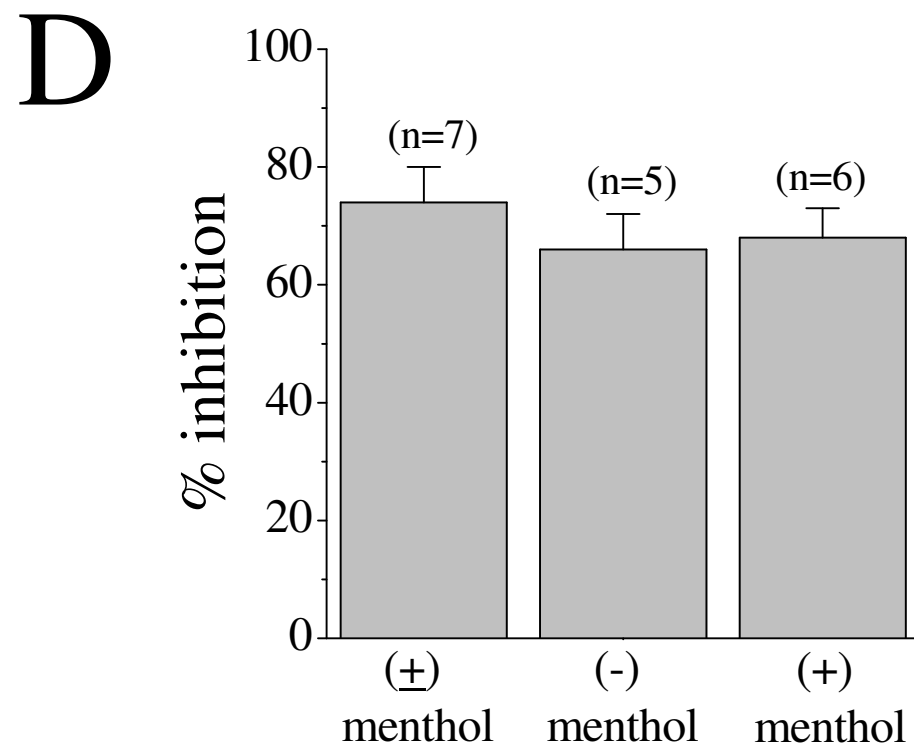
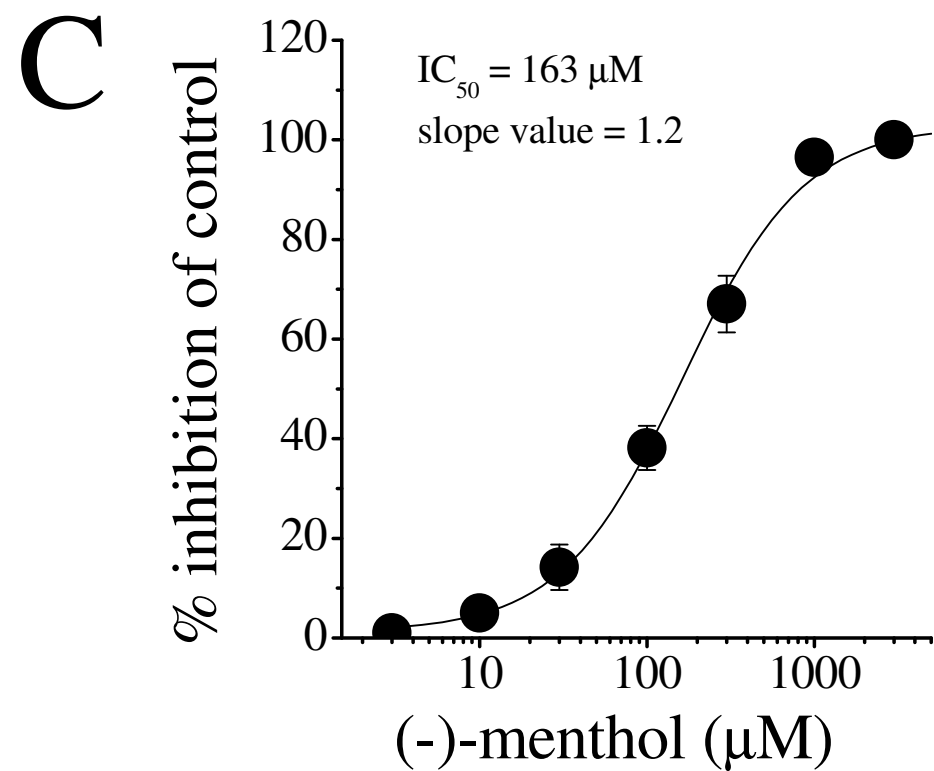
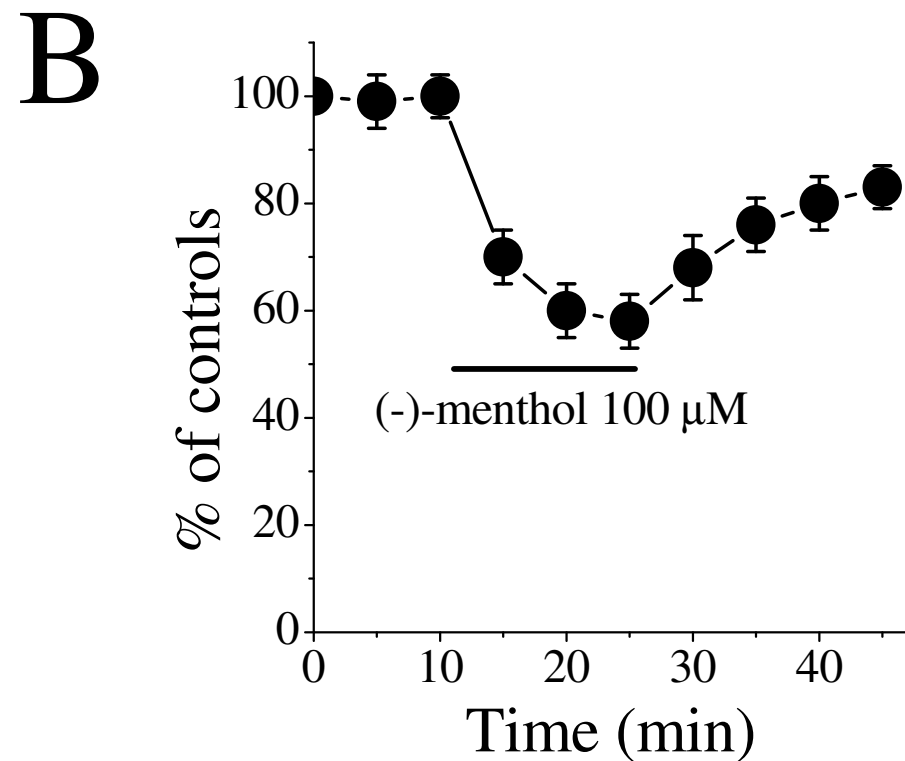
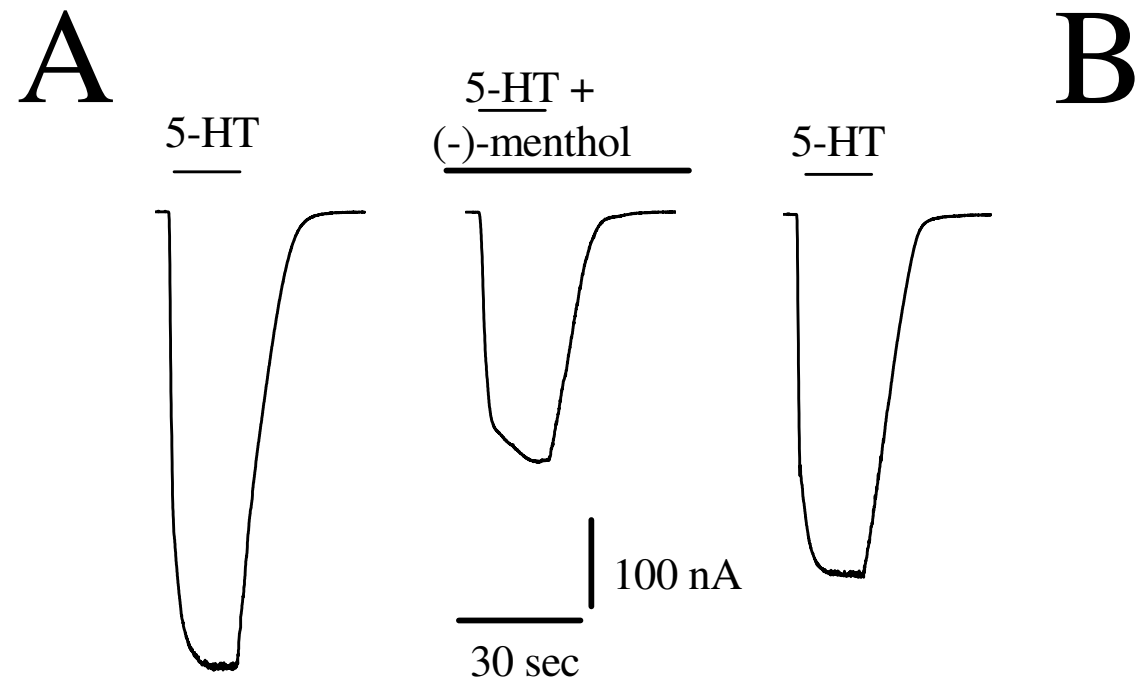
JPET #203976

stabilizes the ligand onto the 5-HTR3A structure is formed with residue THR361 at a distance of 1.81 Å.

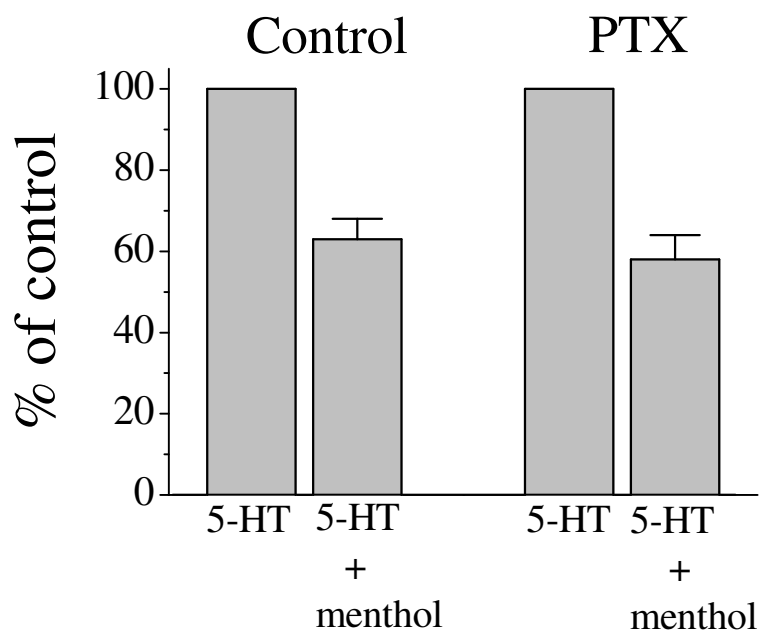
**Table I.**

The effects of menthol (1 mM) on the passive membrane properties of the *Xenopus* oocytes expressing 5-HT<sub>3</sub> receptors.

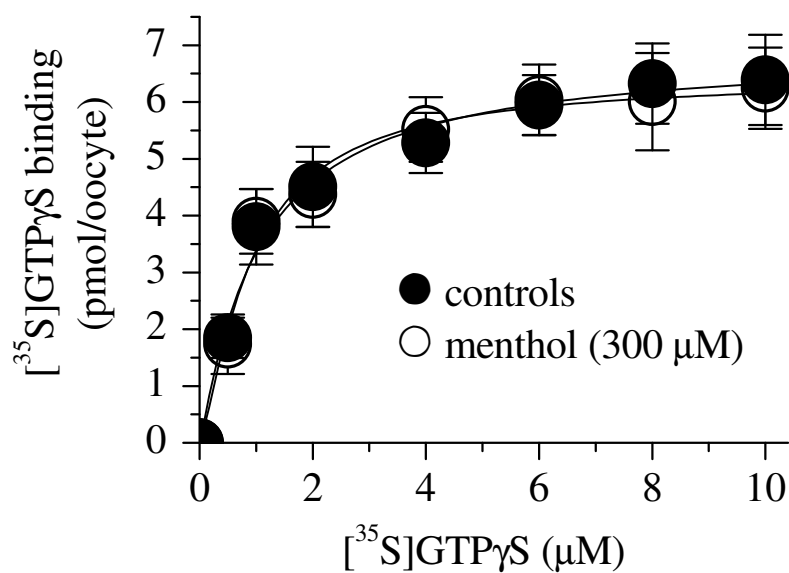
|                       | $R_m$ (M $\Omega$ ) | $C_m$ (nF)   | $V_m$ (mV)      |
|-----------------------|---------------------|--------------|-----------------|
| Control (n=14)        | $1.6 \pm 0.3$       | $223 \pm 27$ | $-42.7 \pm 3.6$ |
| 20 min menthol (n=16) | $1.8 \pm 0.4$       | $218 \pm 15$ | $-39.8 \pm 4.1$ |



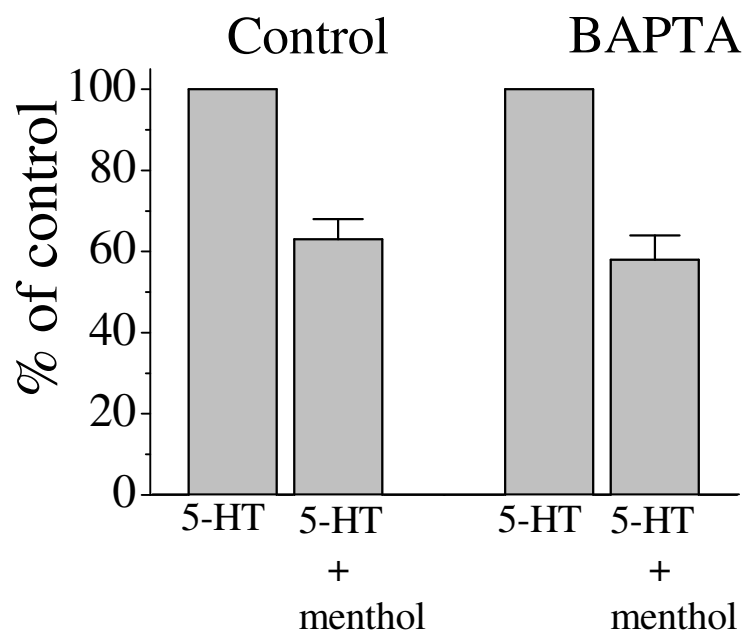
A

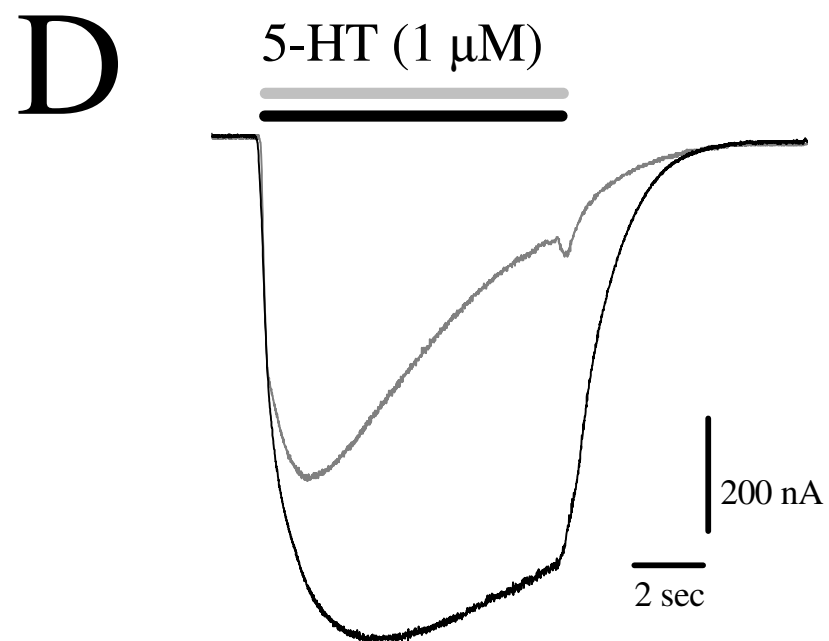
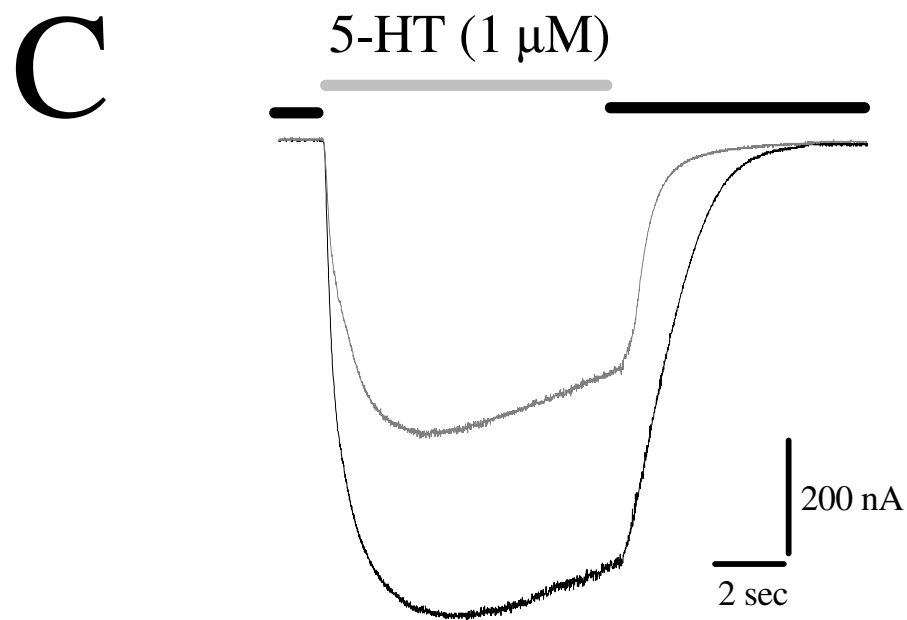
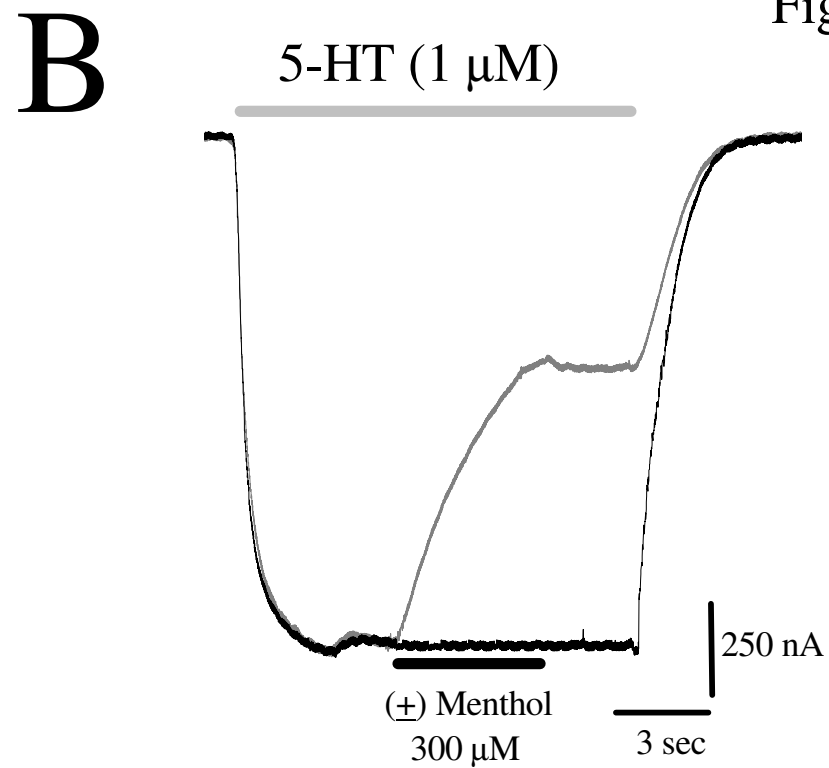
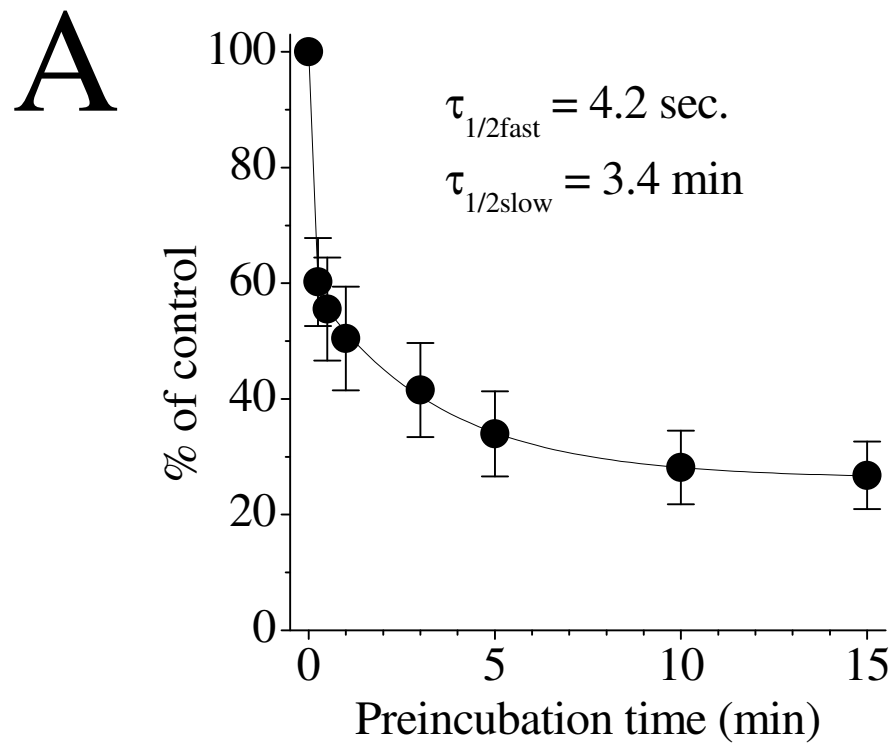


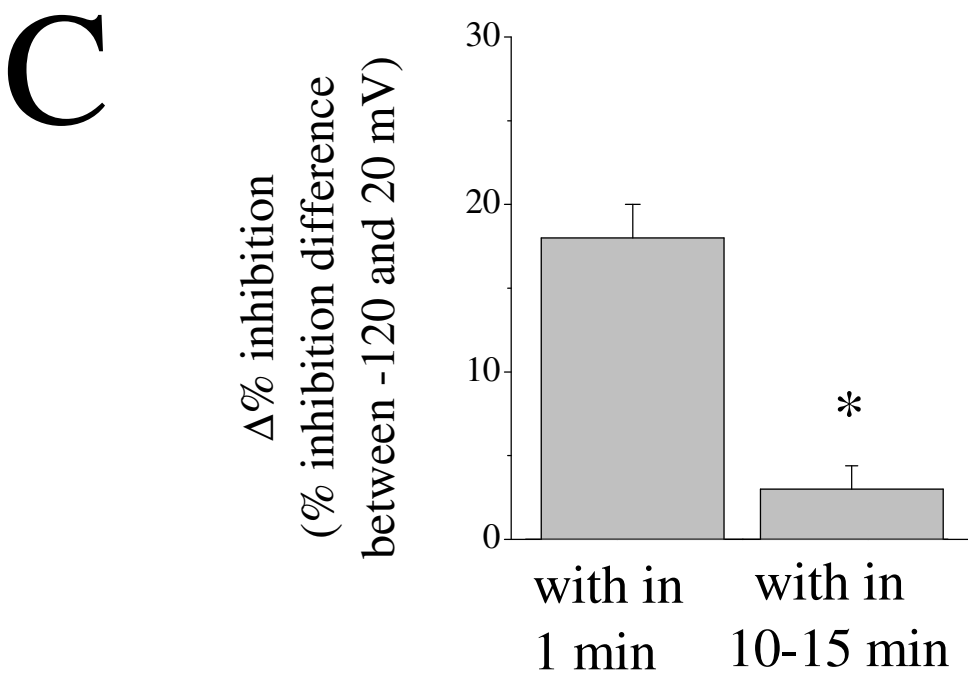
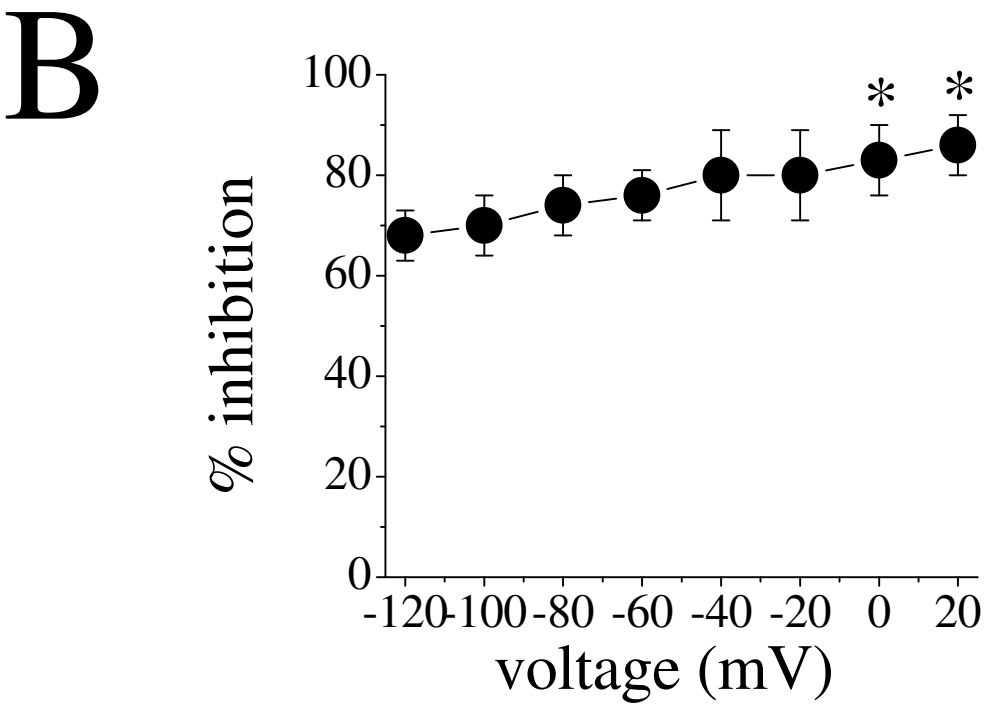
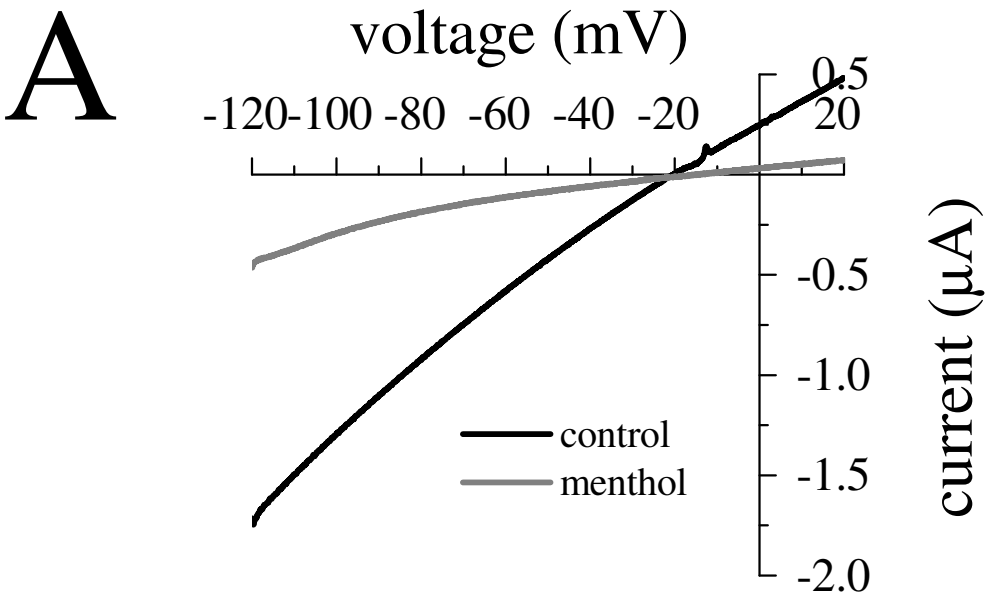
B



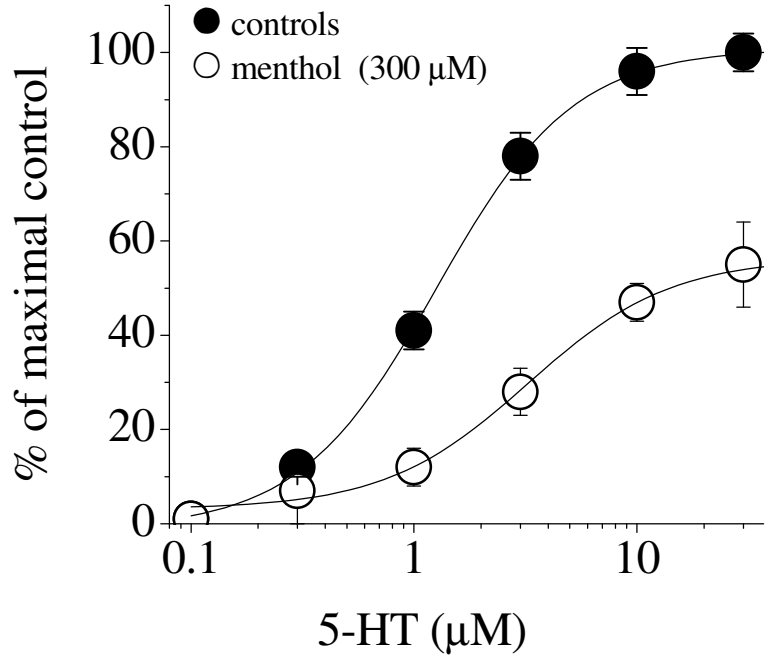
C



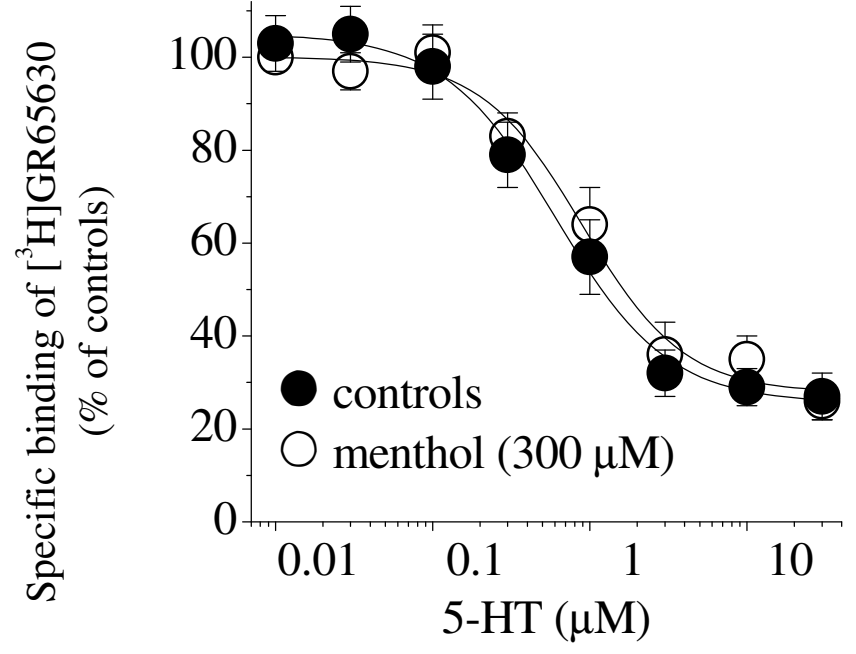




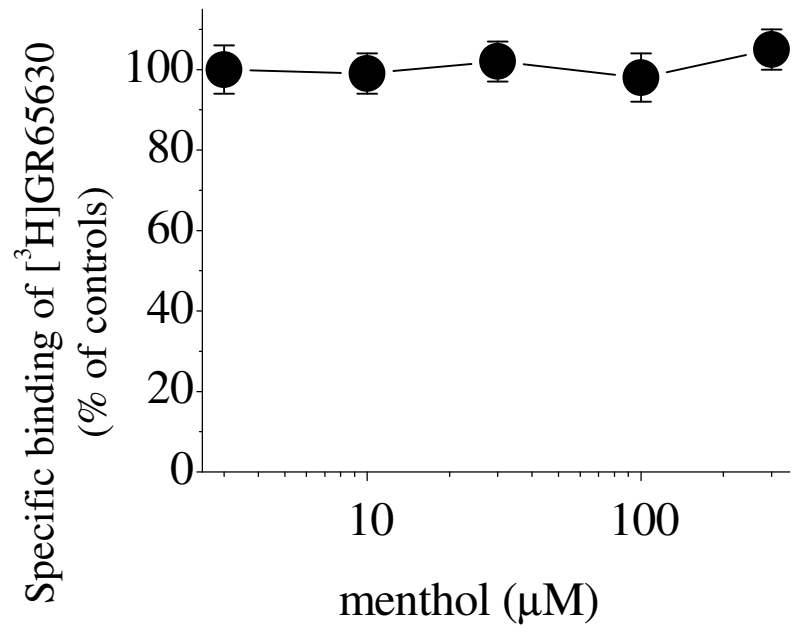
A



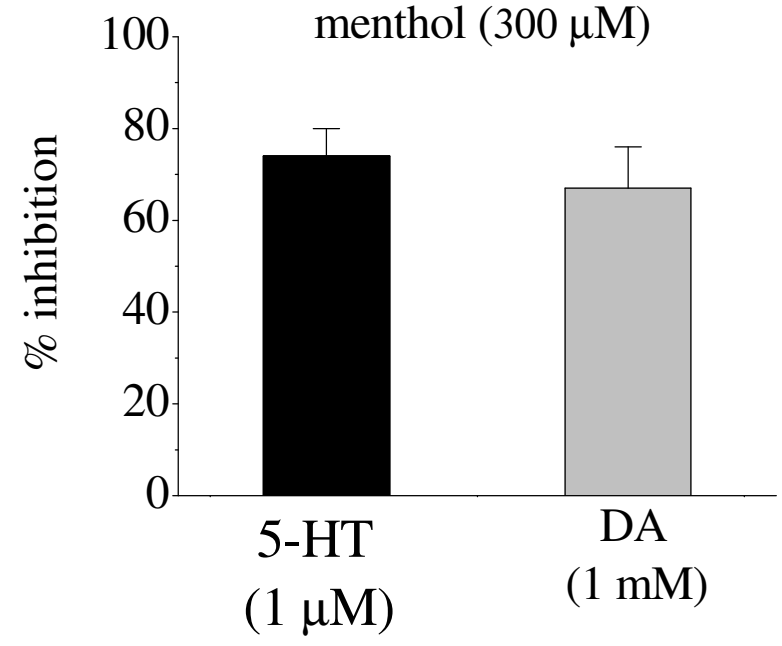
B



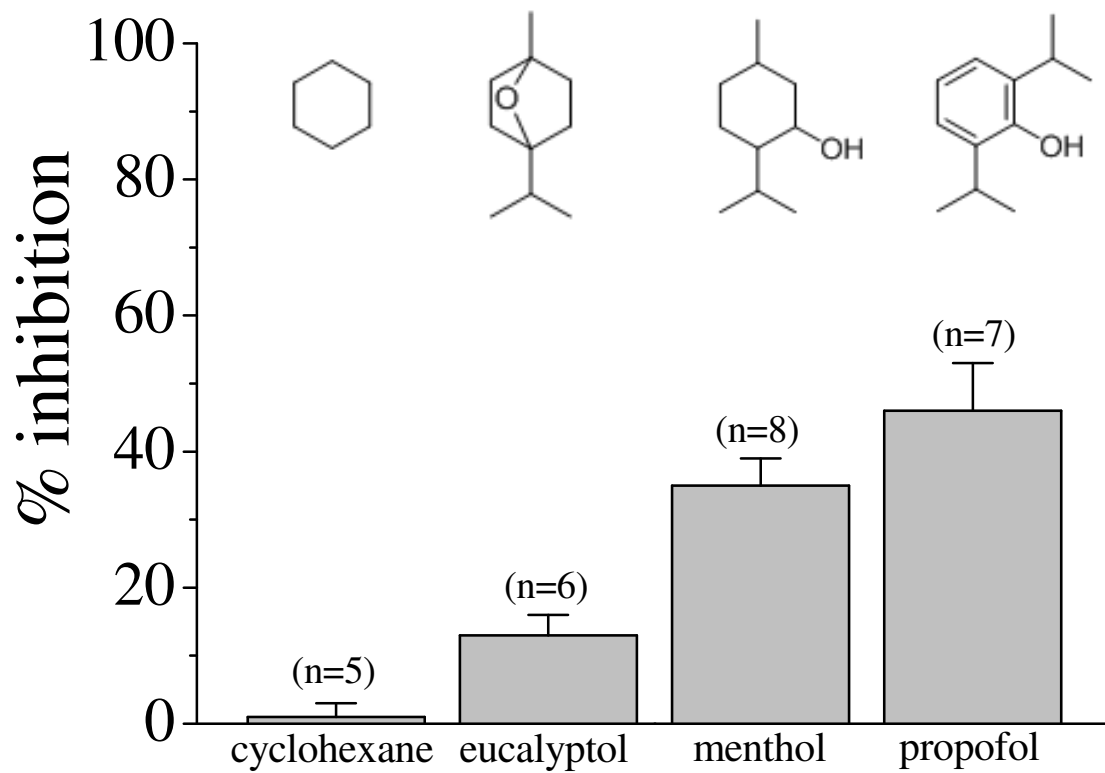
C



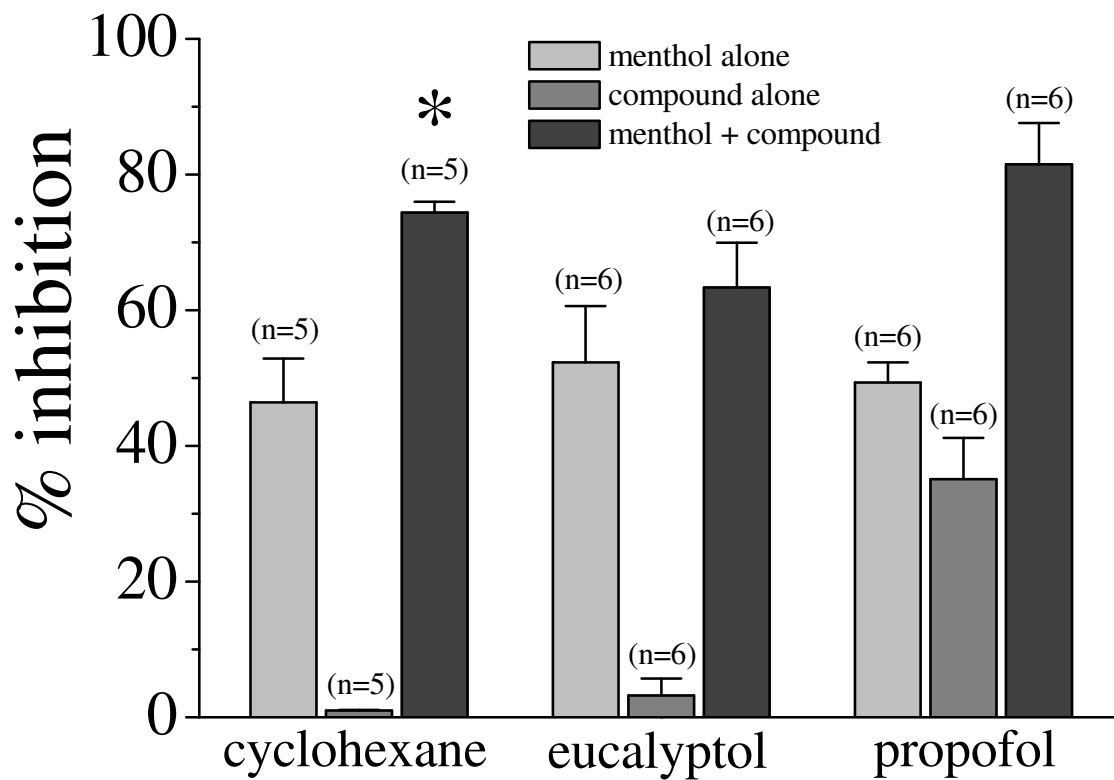
D



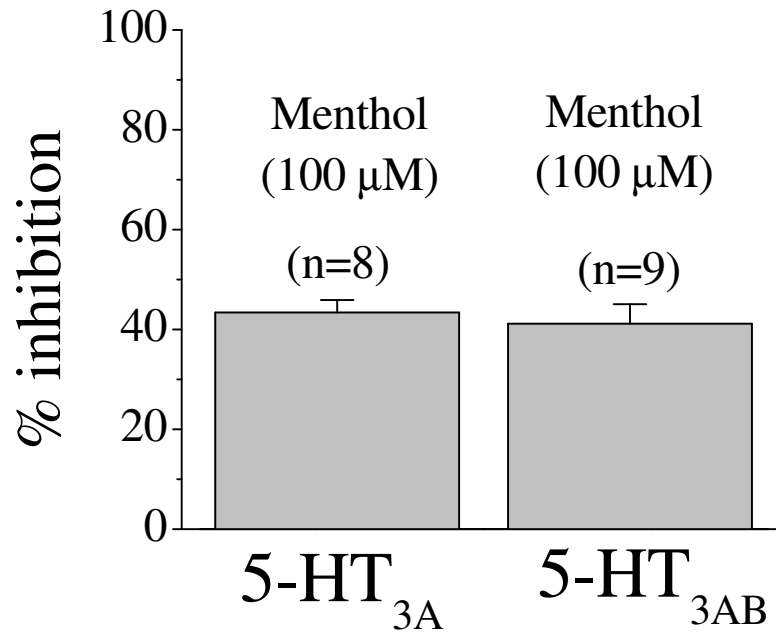
A



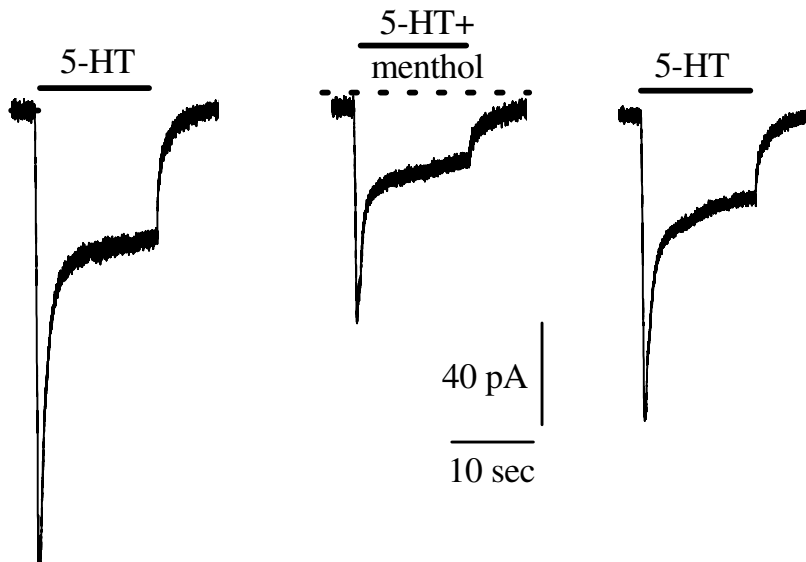
B



A



B

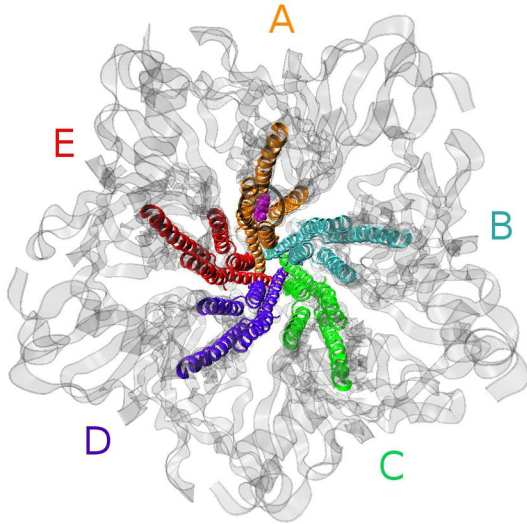


A

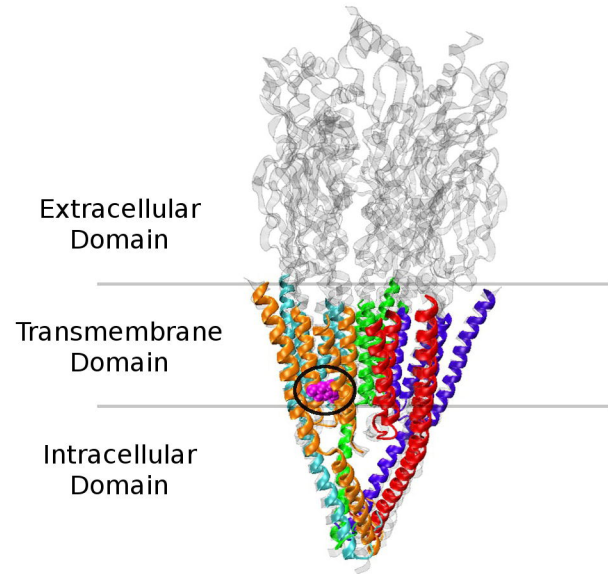
P46098-5 | 5HT3A\_HUMAN  
 2BG9\_A | PDB  
 P14867 | GBRA1\_HUMAN

TGVYFVVCMALLVISLAETIFIVRLVHKQDLQQPVPAWLRHLVLERIAWL 392  
 --KYMLFTMIFVISSIIIVTVVVINTHHR----- 301  
 ---FIAVCYAFVFSALIEFATVNYFTKRG----- 341  
 :: . ::. :: : ::

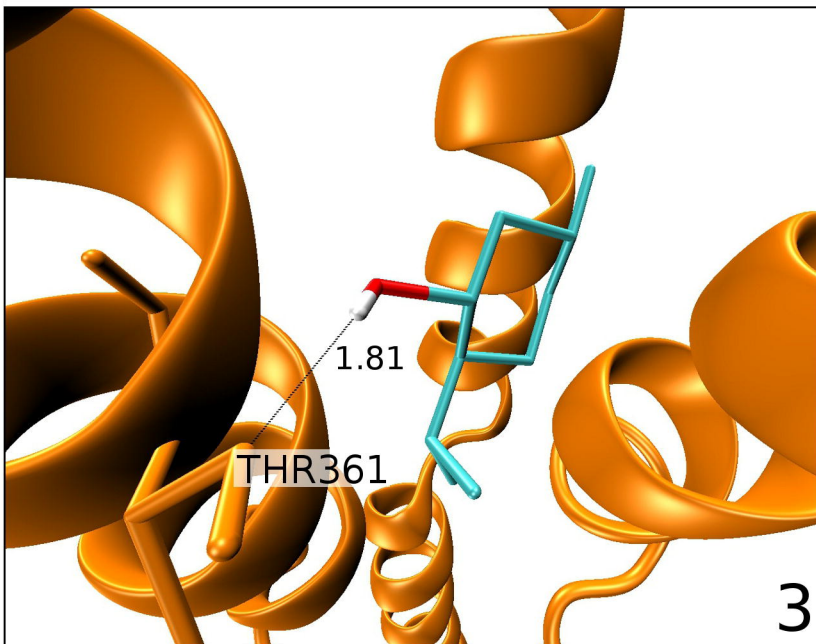
B



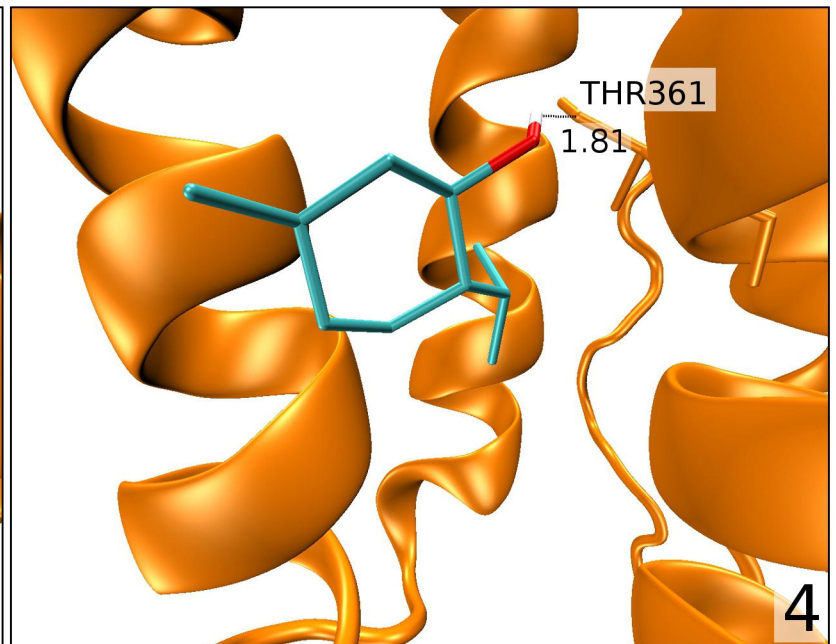
1



2



3



4